Archives of Control Sciences
Volume 12(XLVIII), 2002
No. 1–2, *pages 37–69*

A new control algorithm for a nonholonomic mobile robot

KRZYSZTOF KOZŁOWSKI and JAROSŁAW MAJCHRZAK

In this paper a trajectory tracking control problem for a nonholonomic mobile robot by making use of a kinematic oscillator has been solved. Firstly - time varying oscillator is examined to control nonholonomic mobile robot based only on its kinematics. Secondly - backstepping procedure is proposed to include robot dynamics and servo loop. It is shown that overall multilevel controller is asymptotically globally stable to a small error different from zero. A wide range of simulation results are presented which illustrate behaviour of the controller with respect to tuning its parameters. Some preliminary experiments are reported too.

Key words: mobile robot, nonholonomic constraints, backstepping procedure

1. Introduction

There is a wide literature concerning control of nonholonomic mobile robots published in last ten years [2–4, 10, 14, 16, 19, 23, 27–30], and [21] . The main difficulty in set point stabilization of mobile robots is due to the fact that these systems cannot be stabilized via continuous static feedback which depends on the state. This is due to the Brockett's theorem [5]. Therefore many authors proposed different control schemes to overcome this fundamental difficulty. Among many others propositions there are three main approaches which are proposed in robotics literature. The first one concentrate on using a time-varying control schemes, see for example references [24, 25], and [26]. The second one uses discontinuous control schemes, see for example [1] and [31]. Finally, the third approach named hybrid control scheme, can be considered as a combination of the above two approaches (see work of Young and coauthors [31]). In this paper we refer to works published recently [7, 8], and [9]. Authors of these papers present a general control scheme which uses an idea of oscillator in order to control a nonholonomic mobile robot. This proposition is general in a sense that it allows to solve both set point stabilization and trajectory tracking control problems. We found this approach very attractive due to the fact that it is straightforward to implement and leads to smooth control signals. As a consequence a backstepping procedure can be easily implemented. In [8] it

The authors are with Poznań University of Technology, Institute of Control and Systems Engineering, ul. Piotrowo 3a, 60-965 Poznań, Poland, e-mail: Krzysztof.Kozlowski, Jaroslaw.Majchrzak@put.poznan.pl.

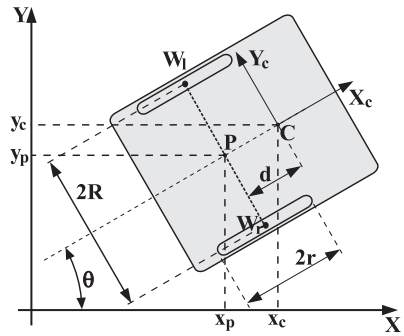

Figure 1. 2-wheeled mobile robot

is proved that the idea of using oscillator to control the kinematics of two wheeled vehicle guarantees global exponential convergence of the tracking error in Cartesian space to a neighbourhood around zero, that can be made arbitrarily small. Based on the kinematic oscillator we propose to consider dynamics of the mobile robot. It is proved in the paper that there is no any initial knowledge required concerning dynamic parameters and uncertainties. Finally, the last backstepping step includes the servo loop. It is shown that the whole system is globally asymptotically stable to a small nonzero error. Unfortunately taking into account dynamics and servo loop of the whole system we lose exponential character of the tracking error convergence to small nonzero error. We believe that this kind of algorithm was not published in a robotics literature and is new. The paper is organized as follows. In section two kinematical consideration are outlined. The third section is devoted to dynamical and servo loop considerations. Section four contains the main backstepping algorithm and its proof. Simulation results are presented in the next section. Some preliminary experimental results are presented too. Concluding remarks end the paper.

2. Kinematics

Consider a 2-wheeled mobile robot shown in Fig. 1. Both wheels have the same radius denoted by r. Width of the vehicle is equal to $2R$. As it is shown in Fig. 1 $\mathbf{XY}$ denotes a base coordinate system. Centre of the mass of the mobile robot is located at point C, which is an origin of the coordinate system $\mathbf{X}_c\mathbf{Y}_c$ assigned to the vehicle. Point P is situated in intersection of a straight line passing through the middle of the vehicle and a section which is an axis of two wheels. Distance between points P and C is denoted by d. Orientation angle is described by θ. Linear velocity of the vehicle at point C is denoted by v while angular velocity around axis passing through point C is ω. It is assumed that wheels roll on the plane $\boldsymbol{XY}$ without longitudinal and transversal

slippage. As a consequence linear velocity vector is perpendicular to the axis joining centre of rotation of both wheels. The first nonholonomic constraint can be written as follows

$$\dot{y}_c \cos\theta - \dot{x}_c \sin\theta - \dot{\theta} d = 0, \tag{1}$$

where $\dot{x}_c$, $\dot{y}_c$ are the velocities of the centre of mass C expressed in the base coordinate system and $\dot{\theta}$ denotes an angular velocity of the vehicle. Note that Eq. (1) represents an algebraic sum of projections of linear and angular velocities on axis connecting centre of both wheels. Equation (1) denotes that the vehicle cannot move in the direction perpendicular to the axis of symmetry of the vehicle. Equivalently Eq. (1) can be rewritten in the following form

$$-\dot{x}_p \sin\theta + \dot{y}_p \cos\theta = \dot{y}_c \cos\theta - \dot{x}_c \sin\theta - d\dot{\theta}. \tag{2}$$

From Eq. (2) it is clear that nonholonomic velocity constraint expressed in point C has the representation which appears on the right side of Eq. (2). At the same time this constraint in point P has the form which appears on the left side of Eq. (2). Next two constraints are called rolling constraints and are as follows (they denote that the driving wheels do not slip)

$$\dot{x}_c \cos\theta + \dot{y}_c \sin\theta + R\dot{\theta} = r\dot{\varphi}_r, \tag{3}$$

$$\dot{x}_c \cos\theta + \dot{y}_c \sin\theta - R\dot{\theta} = r\dot{\varphi}_l, \tag{4}$$

where $\dot{\varphi}_r$ and $\dot{\varphi}_l$ are angular velocities of the right and left wheel, respectively. Equations (3) and (4) are projections of linear and angular velocities (including wheels angular velocities) on $\boldsymbol{X}_c$ axis. Note, that Eq. (3) involves only angular velocity $\dot{\varphi}_r$ while Eq. (4) angular velocity $\dot{\varphi}_l$. Now, introducing a new vector of velocities $\dot{\boldsymbol{q}} = \left[\dot{x}_c\ \dot{y}_c\ \dot{\theta}\ \dot{\varphi}_r\ \dot{\varphi}_l\right]^T$ three constraints (1), (3), and (4) can be rewritten in the following form

$$\boldsymbol{A}(\boldsymbol{q})\dot{\boldsymbol{q}} = \boldsymbol{0}, \tag{5}$$

where

$$\boldsymbol{A}(\boldsymbol{q}) = \begin{bmatrix} -\sin\theta & \cos\theta & -d & 0 & 0 \\ -\cos\theta & -\sin\theta & -R & r & 0 \\ -\cos\theta & -\sin\theta & R & 0 & r \end{bmatrix}. \tag{6}$$

One can easly calculate [30] that among the three constraints, two of then are nonholonomic and the third one is holonomic. In order to calculate the holonomic constraint, we subtract Eq. (4) from Eq. (3) which gives

$$2R\dot{\theta} = r\left(\dot{\varphi}_r - \dot{\varphi}_l\right). \tag{7}$$

Clearly integrating the above equation one can get

$$\theta = c(\varphi_r - \varphi_l) + constant, \tag{8}$$

which is a holonomic constraint, where $c = \frac{r}{2R}$. Last equation has a nice physical interpretation, namely the heading angle of the vehicle is determined by the relative difference between two wheels. It is easy to calculate $\dot{\varphi}_r$ from Eq. (7)

$$\dot{\varphi}_r = \frac{2R\dot{\theta} + r\dot{\varphi}_l}{r}. \tag{9}$$

Substitution of (9) into Eq. (3) gives $\dot{x}_c \cos\theta + \dot{y}_c \sin\theta - R\dot{\theta} = r\dot{\varphi}_l$ which is exactly the third nonholonomic constraint (compare Eq. (4)). As a consequence, taking into account Eqs. (7) and (9), two nonholonomic and one holonomic constraints can be rewritten as follows

$$\boldsymbol{A}_1(\boldsymbol{q})\dot{\boldsymbol{q}} = \begin{bmatrix} -\sin\theta & \cos\theta & -d & 0 & 0 \\ -\cos\theta & -\sin\theta & -R & r & 0 \\ 0 & 0 & -2R & r & -r \end{bmatrix} \dot{\boldsymbol{q}} = \boldsymbol{0}. \tag{10}$$

Since the constrained velocity is always in the null space of $\boldsymbol{A}(\boldsymbol{q})$, it is possible to define $(n-m)$ velocities $\boldsymbol{\nu} = [\nu, \ldots, \nu_{n-m}]^T$ such that (these velocities need not be integrable)

$$\dot{\boldsymbol{q}} = \boldsymbol{S}(\boldsymbol{q})\boldsymbol{\nu}, \tag{11}$$

where n is the dimension of vector $\boldsymbol{q}$ and m is a total number of holonomic and nonholonomic constraints. Matrix $\boldsymbol{S}(\boldsymbol{q})$ has full rank and satisfies $\boldsymbol{A}(\boldsymbol{q})\boldsymbol{S}(\boldsymbol{q}) = \boldsymbol{0}$. In our case $n = 5$ and $m = 3$ (two nonholonomic and one holonomic constraints) and we have $\boldsymbol{\nu} = [\dot{\varphi}_r \ \dot{\varphi}_l]^T$. It is easy to verify (from geometrical considerations concerning appropriate velocities) that there exists the following relationship between linear and angular velocities of the vehicle and wheels' velocities

$$\boldsymbol{\nu} = \begin{bmatrix} \dot{\varphi}_r \\ \dot{\varphi}_l \end{bmatrix} = \begin{bmatrix} \frac{1}{r} & \frac{1}{2c} \\ \frac{1}{r} & -\frac{1}{2c} \end{bmatrix} \begin{bmatrix} v \\ \omega \end{bmatrix}. \tag{12}$$

A square matrix which appears in the last equation is nonsingular, therefore it is not of importance which velocities we use to describe the kinematics of the vehicle considered in this paper. Substitution of Eq. (12) into Eq. (11) results

$$\dot{\boldsymbol{q}} = \begin{bmatrix} \cos\theta & -d\sin\theta \\ \sin\theta & d\cos\theta \\ 0 & 1 \\ \frac{1}{r} & \frac{1}{2c} \\ \frac{1}{r} & -\frac{1}{2c} \end{bmatrix} \begin{bmatrix} v \\ \omega \end{bmatrix} = \boldsymbol{S}_1(\boldsymbol{q}) \begin{bmatrix} v \\ \omega \end{bmatrix}. \tag{13}$$

Now we skip last two equations from Eq. (13) and rewrite it as follows

$$\dot{\boldsymbol{q}}_1 = \begin{bmatrix} \dot{x}_c \\ \dot{y}_c \\ \dot{\theta} \end{bmatrix} = \begin{bmatrix} \cos\theta & -d\sin\theta \\ \sin\theta & d\cos\theta \\ 0 & 1 \end{bmatrix} \begin{bmatrix} v \\ \omega \end{bmatrix} = \boldsymbol{S}_2(\boldsymbol{q}_1)\boldsymbol{\nu}, \tag{14}$$

where $\dot{\boldsymbol{q}}_1 = [\dot{x}_c\ \dot{y}_c\ \dot{\theta}]^T$ and here $\boldsymbol{\nu} = [v\ \omega]^T$. Notice that equations (12) and (14) constitute Eq. (13). Matrix $\boldsymbol{A}_2(\boldsymbol{q}_1)$ which satisfies equation $\boldsymbol{A}_2(\boldsymbol{q}_1)\boldsymbol{S}_2(\boldsymbol{q}_1) = \boldsymbol{0}$ has the following form

$$\boldsymbol{A}_2(\boldsymbol{q}_1) = [\ -\sin\theta \quad \cos\theta \quad -d\ ] \tag{15}$$

and certainly $\boldsymbol{A}_2(\boldsymbol{q}_1)\dot{\boldsymbol{q}}_1 = \boldsymbol{0}$ results in

$$-\dot{x}_c \sin\theta + \dot{y}_c \cos\theta - d\dot{\theta} = 0 \tag{16}$$

which has exactly the same form as Eq. (1) (first nonholonomic constraint). Note that in case of Eq. (13) we still have the same number of constraints, one holonomic and two nonholonomic, while in case of Eq. (14) we are dealing with only one nonholonomic constraint.

3. Dynamics

In this section we describe dynamics of the vehicle presented in Fig. 1. In general the dynamical model of a mobile robot is given by

$$\boldsymbol{M}(\boldsymbol{q})\ddot{\boldsymbol{q}} + \boldsymbol{V}_m(\boldsymbol{q},\dot{\boldsymbol{q}})\dot{\boldsymbol{q}} + \boldsymbol{F}(\dot{\boldsymbol{q}}) + \boldsymbol{G}(\boldsymbol{q}) + \boldsymbol{\tau}_z = \boldsymbol{B}(\boldsymbol{q})\boldsymbol{\tau} - \boldsymbol{A}^T(\boldsymbol{q})\boldsymbol{\lambda}, \tag{17}$$

where $\boldsymbol{M}(\boldsymbol{q})$ is a symmetric, positive definite matrix, $\boldsymbol{V}_m$ is a centripetal and Coriolis matrix, $\boldsymbol{F}$ is a friction vector, $\boldsymbol{G}$ is a gravity vector, $\boldsymbol{\tau}_d$ is a vector of disturbances including unmodeled dynamics, $\boldsymbol{B}$ is an input transformation matrix, $\boldsymbol{\tau}$ is a control input vector, $\boldsymbol{A}$ is a matrix associated with constraints, and $\boldsymbol{\lambda}$ is a vector of constraint forces. The dynamics of the driving and steering motors should be included in the robot dynamics along with the mechanical gearing. Since in our case robot moves on a plane, vector $\boldsymbol{G} = \boldsymbol{0}$. Vector $\boldsymbol{q}$ describes a vector of coordinates, and consequently $\dot{\boldsymbol{q}}$ and $\ddot{\boldsymbol{q}}$ denote velocity and acceleration vectors, respectively. Matrix $\boldsymbol{A}^T(\boldsymbol{q})$ which appears in Eq. (17) is of the form of Eq. (15) in the case considered here.

Now we derive in a systematic way, the left hand side of Eq. (17). First, we formulate Lagrangian of the system which is defined as follows

$$L(\boldsymbol{q},\dot{\boldsymbol{q}}) = E_k(\boldsymbol{q},\dot{\boldsymbol{q}}) - E_p(\boldsymbol{q}), \tag{18}$$

where $E_k(\boldsymbol{q},\dot{\boldsymbol{q}})$ stands for a kinetic energy and $E_p(\boldsymbol{q})$ is a potential energy which in our case is equal to zero. Kinetic energy of the vehicle has the following form

$$E_{kv} = \frac{1}{2}m_0 v^2 + \frac{1}{2}J_0\omega^2, \tag{19}$$

where v denotes a linear velocity of the vehicle and ω is an angular velocity. Mass of the vehicle (without mass of the wheels) is denoted by m_0 and J_0 is a moment of inertia

around axis passing through point P. Now observing that $\dot{\theta} = \omega$ and using velocities of points P and C in Fig. 1. Eq. (19) can be rewritten in the following form

$$E_{kv} = \frac{1}{2} m_0 \left(\dot{x}_c^2 + \dot{y}_c^2\right) + m_0 \dot{\theta} d \left(\dot{x}_c \sin\theta - \dot{y}_c \cos\theta\right) + \frac{1}{2} m_0 d^2 \dot{\theta}^2 + \frac{1}{2} J_0 \dot{\theta}^2, \tag{20}$$

where we have used fact that $v = \sqrt{\dot{x}_p^2 + \dot{y}_p^2}$. Now we formulate kinetic energy of the right and left wheel, respectively

$$\begin{aligned} E_{kr} &= \tfrac{1}{2} \left(m_{wr} v_r^2 + A_{kr} \omega^2 + C_{nr} \dot{\varphi}_r^2\right), \\ E_{kl} &= \tfrac{1}{2} \left(m_{wl} v_l^2 + A_{kl} \omega^2 + C_{nl} \dot{\varphi}_l^2\right), \end{aligned} \tag{21}$$

where m_{wr} and m_{wl} denote mass of the right and left wheel including mass of the right and left actuator, A_{kr} and A_{kl} are the moment of inertia of the right and left wheel about a diameter, respectively. Finally, C_{nr} and C_{nl} denote the right and left axial moment of inertia including the actuators inertia. v_r and v_l are linear velocities of right and left wheel, respectively, which are calculated as follows $v_r = r\dot{\varphi}_r$ and $v_l = r\dot{\varphi}_l$. Assuming that, $m_{wr} = m_{wl} = m_w$, $C_{nr} = C_{nl} = C_n$, $A_{kr} = A_{kl} = A_k$ total energy of the wheels can be rewritten as follows

$$E_{kr} + E_{kl} = \frac{1}{2} \left[m_w \left(v_r^2 + v_l^2\right) + 2A_k \dot{\theta}^2\right] + + \frac{1}{2} \left[C_n \left(\dot{\varphi}_r^2 + \dot{\varphi}_l^2\right)\right]. \tag{22}$$

In order to calculate linear velocity of point W_r and W_l as indicated in Fig. 1 notice that coordinates of points W_l are as follows

$$y_{wl} = y_c - d\sin\theta + R\cos\theta, \tag{23}$$

$$x_{wr} = x_c - d\cos\theta - R\sin\theta. \tag{24}$$

Differentiating the above equations gives

$$\dot{y}_{wl} = \dot{y}_c - d\dot{\theta}\cos\theta - R\dot{\theta}\sin\theta, \tag{25}$$

$$\dot{x}_{wr} = \dot{x}_c + d\dot{\theta}\sin\theta - R\dot{\theta}\cos\theta. \tag{26}$$

Now one can easily calculate

$$\begin{aligned} v_l^2 + v_r^2 = \dot{\varphi}_l^2 r^2 + \dot{\varphi}_r^2 r^2 = \dot{y}_{wl}^2 + \dot{x}_{wl}^2 + \dot{y}_{wr}^2 + \dot{x}_{wr}^2 = \\ 2(\dot{x}_c^2 + \dot{y}_c^2) + 2(d^2 + R^2)\dot{\theta}^2 - 4\dot{y}_c\dot{\theta}d\cos\theta + 4\dot{x}_c\dot{\theta}d\sin\theta. \end{aligned} \tag{27}$$

Substitution of Eq. (27) in Eq. (22) gives

$$\begin{aligned} E_{kr} + E_{kl} = \tfrac{1}{2} \left(2m_w + 2\tfrac{C_n}{r^2}\right) \left(\dot{x}_c^2 + \dot{y}_c^2\right) + \left(d^2 + R^2\right) \dot{\theta}^2 \left(m_w + C_n \tfrac{1}{r^2}\right) + \\ m_w d\dot{\theta} \left(\dot{x}_c \sin\theta - \dot{y}_c \cos\theta\right) + A_k \dot{\theta}^2. \end{aligned} \tag{28}$$

Total energy of the vehicle can be calculated based on Eqs. (20) and (28) as follows

$$E_k = \frac{1}{2}\left(m_0 + 2m_w + 2\frac{C_n}{r^2}\right)\left(\dot{x}_c^2 + \dot{y}_c^2\right) + d\dot{\theta}^2\left(m_0 + 2m_w + 2C_n\frac{1}{r^2}\right)\left(\dot{x}_c\sin\theta - \dot{y}_c\cos\theta\right)$$
$$+\frac{1}{2}\dot{\theta}^2\left[J_0 + m_o d^2 + 2A_k + 2\left(d^2 + R^2\right)\left(m_w + C_n\frac{1}{r^2}\right)\right]. \tag{29}$$

Now we introduce the following notation $m = m_0 + 2m_w + 2\frac{C_n}{r^2}$ and $J = J_0 + m_0 d^2 + 2A_k + 2\left(m_w + C_n\frac{1}{r^2}\right)\left(d^2 + R^2\right)$ and rewrite Eq. (29) as

$$E_k = \frac{1}{2}m\left(\dot{x}_c^2 + \dot{y}_c^2\right) + md\dot{\theta}\left(\dot{x}_c\sin\theta - \dot{y}_c\cos\theta\right) + \frac{1}{2}J\dot{\theta}^2. \tag{30}$$

Here we make one comment. Note that constraint equations are not used in deriving wheel and mobile base kinetic energy. Constraints are imposed on dynamic equations later using Lagrange multipliers. In another words, one should have a set of motion equations even if constraints are not satisfied.

Notice that the total energy is expressed in terms of generalized positions x_c, y_c, θ and their time derivatives. The case considered here is equivalent to the situation when inertia of the wheels and actuators is equivalent to the mass which sums up with the mass of the wheels. In practice there are no drives mounted along the wheels and one pushes the vehicle so the wheels roll without slipping (it is assumed that the drives are idle). Next we construct matrix $\boldsymbol{B}(\boldsymbol{q})$ which appears in Eq. (17). This matrix is called an input transformation matrix. Recall that two moments τ_r and τ_l, act on the right and left wheel, respectively. Namely, these are torques acting on the wheels of the vehicle. Motor torques will be included later in this section. There are two generalized forces acting on a vehicle, one of them is force, F_v, which moves it with linear velocity v and the second one is the moment of force, M_v, causing movement of the vehicle with angular velocity ω. Mathematically these generalized forces can be written as follows

$$F_v = \frac{1}{r}\left(\tau_r + \tau_l\right), \qquad M_v = \frac{R}{r}\left(\tau_r - \tau_l\right) \tag{31}$$

assuming that they are expressed in the base coordinate system. In more compact form one can write

$$\boldsymbol{\tau}_v = \begin{bmatrix} F_v \\ M_v \end{bmatrix} = \begin{bmatrix} \frac{1}{r} & \frac{1}{r} \\ \frac{R}{r} & -\frac{R}{r} \end{bmatrix}\begin{bmatrix} \tau_r \\ \tau_l \end{bmatrix} = \bar{\boldsymbol{B}}(\boldsymbol{q})\boldsymbol{\tau}. \tag{32}$$

Since all calculations are done in the base coordinate system force F_v is projected on $\boldsymbol{X}$ and $\boldsymbol{Y}$ axes, therefore one can write

$$\begin{bmatrix} F_{vx} \\ F_{vy} \\ M_v \end{bmatrix} = \frac{1}{r}\begin{bmatrix} \left(\tau_r + \tau_l\right)\cos\theta \\ \left(\tau_r + \tau_l\right)\sin\theta \\ R\left(\tau_r - \tau_l\right) \end{bmatrix} = \boldsymbol{B}\begin{bmatrix} \tau_r \\ \tau_l \end{bmatrix}, \tag{33}$$

where the input transformation matrix $\boldsymbol{B}$ has the following form

$$\boldsymbol{B} = \frac{1}{r}\begin{bmatrix} \cos\theta & \cos\theta \\ \sin\theta & \sin\theta \\ R & -R \end{bmatrix}. \tag{34}$$

Now we calculate all partial and time derivatives of the kinetic given by Eq. (30) according to the Lagrange principle which result in the following equations of motion

$$m\ddot{x}_c + md\ddot{\theta}\sin\theta + md\dot{\theta}^2\cos\theta + F_x(\dot{\boldsymbol{q}}) + \tau_{zx} = \frac{1}{r}(\tau_r + \tau_l)\cos\theta + \lambda\sin\theta, \tag{35}$$

$$m\ddot{y}_c - md\ddot{\theta}\cos\theta + md\dot{\theta}^2\sin\theta + F_y(\dot{\boldsymbol{q}}) + \tau_{zy} = \frac{1}{r}(\tau_r + \tau_l)\sin\theta - \lambda\cos\theta, \tag{36}$$

$$md\ddot{x}_c\sin\theta - md\ddot{y}_c\cos\theta + J\ddot{\theta} + F_\theta(\dot{\boldsymbol{q}}) + \tau_{z\theta} = \frac{R}{r}(\tau_r - \tau_l) + \lambda d \tag{37}$$

where $F_x(\dot{\boldsymbol{q}})$, $F_y(\dot{\boldsymbol{q}})$, $F_\theta(\dot{\boldsymbol{q}})$ and τ_{zx}, τ_{zy}, $\tau_{z\theta}$ are coordinates of vectors $\boldsymbol{F}(\dot{\boldsymbol{q}})$ and $\boldsymbol{\tau}_z$,

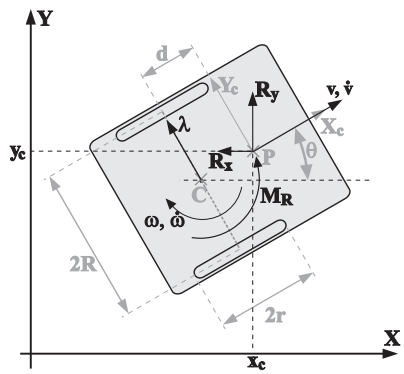

Figure 2. Reaction forces on $\mathbf{XY}$ plane

respectively. It is clear from Eqs. (35)-(37) that the mass matrix of the vehicle can be written as follows

$$\boldsymbol{M}(\boldsymbol{q}) = \begin{bmatrix} m & 0 & md\sin\theta \\ 0 & m & -md\cos\theta \\ md\sin\theta & -md\cos\theta & J \end{bmatrix}, \tag{38}$$

and the centripetal and Coriolis matrix $\boldsymbol{V}_m(\boldsymbol{q}, \dot{\boldsymbol{q}})$ is of the form

$$\boldsymbol{V}_m(\boldsymbol{q}, \dot{\boldsymbol{q}}) = \begin{bmatrix} 0 & 0 & md\dot{\theta}\cos\theta \\ 0 & 0 & md\dot{\theta}\sin\theta \\ 0 & 0 & 0 \end{bmatrix}. \tag{39}$$

Note, that in the equations of motion (Eqs. (35)-(37)) one Lagrange multiplier appears which is consistent with the fact that in the system considered here three coordinates are present. In order to calculate it we assume that two components $\boldsymbol{F}(\dot{\boldsymbol{q}})$ and $\boldsymbol{\tau}_z$ are not present in Eqs. (35)-(37). We multiply Eq. (35) by $\sin\theta$ and Eq. (36) by $-\cos\theta$, and sum both sides of these equations. As a result we get

$$\lambda = m\left(\ddot{x}_c \sin\theta - \ddot{y}_c \cos\theta\right) + md\ddot{\theta}. \tag{40}$$

In order to eliminate accelerations which appear in this equation (to obtain a simpler form for λ) one can differentiate Eq. (16) and multiply by m

$$-m\ddot{x}_c \sin\theta - m\dot{x}_c\dot{\theta}\cos\theta + m\ddot{y}_c \cos\theta + -m\dot{y}_c\dot{\theta}\sin\theta - md\dot{\theta} = 0. \tag{41}$$

Using Eq. (41) in Eq. (40) we get

$$\lambda = -m\dot{\theta}\left(\dot{x}_c \cos\theta + \dot{y}_c \sin\theta\right). \tag{42}$$

In order to illustrate the constraint forces consider a situation presented in Fig. 2. In this figure vector of constraint force is perpendicular to the wheels. Its coordinates in the base coordinate system can be calculated as follows

$$\begin{bmatrix} R_x \\ R_y \\ M_R \end{bmatrix} = \begin{bmatrix} -\lambda\sin\theta \\ \lambda\cos\theta \\ -\lambda d \end{bmatrix}. \tag{43}$$

Components of this vector are illustrated in Fig. 2. Note that one can obtain the same result calculating expression $\boldsymbol{A}^T\lambda$ which appears on the right hand side of Eq. (17). Moment force, M_R, is acting due to the fact that points P and C do not coincide. Another observation is that the constraint force λ represents Coulomb friction acting along the axis of both wheels. Clearly the Coulomb friction force $\boldsymbol{T}_C$ has two components in the base coordinate system which are expressed by the first two components of Eq. (43). Now it is quite easy to estimate the static friction coefficient taking into account load force of the vehicle exerted on the ground on which it moves. Namely this force equals $\boldsymbol{F}_N = m\boldsymbol{g}$, where $\boldsymbol{g}$ is the gravity vector. Notice that the same mass appears in Eq. (42). Based on this observation one can calculate value of the maximal transverse friction force which causes transverse sliding of the vehicle as follows

$$\boldsymbol{T}_C \leqslant \mu_N \boldsymbol{F}_N, \tag{44}$$

where μ_N denotes friction coefficient. Note that when this inequality is not satisfied we are not able to control the nonholonomic robot by using methods discussed later in this paper.

Equations of motion (35)-(37) correspond to generalized positions x_c, y_c and θ. One can write down equations of motion in terms of coordinates given by vector $\boldsymbol{q} = [x_c\ y_c\ \theta\ \varphi_r\ \varphi_l]^T$. Kinetic energy of the vehicle has the following form

$$\begin{aligned} E_k = {} & \tfrac{1}{2}(m_0 + 2m_w)\left(\dot{x}_c^2 + \dot{y}_c^2\right) + d\dot{\theta}(m_0 + 2m_w)\left(\dot{x}_c\sin\theta - \dot{y}_c\cos\theta\right) + \\ & + C_n\left(\dot{\varphi}_r^2 + \dot{\varphi}_l^2\right) + \tfrac{1}{2}\dot{\theta}^2\left[J + m_0 d^2 + 2A_k + 2\left(d^2 + R^2\right)\right]. \end{aligned} \tag{45}$$

Now we introduce the following notation $m_1 = m_0 + 2m_w$ and $J_1 = J_0 + m_0 d^2 + 2A_k + 2m_w(d^2 + R^2)$ and rewrite kinetic energy as follows

$$E_k = \frac{1}{2} m_1 \left(\dot{x}_c^2 + \dot{y}_c^2\right) + d\dot{\theta} m_1 \left(\dot{x}_c \sin\theta - \dot{y}_c \cos\theta\right) + C_n \left(\dot{\varphi}_r^2 + \dot{\varphi}_l^2\right) + \frac{1}{2}\dot{\theta}^2 J_1. \quad (46)$$

Note that the kinematic energy given by Eq. (46) has the same structure as kinetic energy expressed by Eq. (30) exept the third term which appears explicitly due to the fact that vector of coordinates includes now angular velocities of both wheels.

Taking into account matrix $\boldsymbol{A}(\boldsymbol{q})$ given by Eq. (6) the equations of motion in this case have the following form

$$\begin{gathered}
m_1 \ddot{x}_c + m_1 d\ddot{\theta} \sin\theta + m_1 d\dot{\theta}^2 \cos\theta + F_x(\dot{\boldsymbol{q}}) + \tau_{zx} = \lambda_1 \sin\theta + (\lambda_2 + \lambda_3)\cos\theta, \\
m_1 \ddot{y}_c - m_1 d\ddot{\theta} \cos\theta + m_1 d\dot{\theta}^2 \sin\theta + F_y(\dot{\boldsymbol{q}}) + \tau_{zy} = -\lambda_1 \cos\theta + (\lambda_2 + \lambda_3)\sin\theta, \\
m_1 d\ddot{x}_c \sin\theta - m_1 d\ddot{y}_c \cos\theta + J_1 \ddot{\theta} + F_\theta(\dot{\boldsymbol{q}}) + \tau_{z\theta} = \lambda_1 d - (\lambda_3 - \lambda_2) R, \\
C_n \ddot{\varphi}_r + F_{\varphi_r}(\dot{\boldsymbol{q}}) + \tau_{z\varphi_r} = -r\lambda_2 + \tau_r, \\
C_n \ddot{\varphi}_l + F_{\varphi_l}(\dot{\boldsymbol{q}}) + \tau_{z\varphi_l} = -r\lambda_3 + \tau_l.
\end{gathered} \quad (47)$$

Based on the above equations matrices $\boldsymbol{M}(\boldsymbol{q})$, $\boldsymbol{V}_m(\boldsymbol{q}, \dot{\boldsymbol{q}})$, and $\boldsymbol{B}(\dot{\boldsymbol{q}})$ are as follows

$$\boldsymbol{M}(\boldsymbol{q}) = \begin{bmatrix} m_1 & 0 & m_1 d\sin\theta & 0 & 0 \\ 0 & m_1 & -m_1 d\cos\theta & 0 & 0 \\ m_1 d\sin\theta & -m_1 d\cos\theta & J_1 & 0 & 0 \\ 0 & 0 & 0 & C_n & 0 \\ 0 & 0 & 0 & 0 & C_n \end{bmatrix},$$

$$\boldsymbol{V}_m(\boldsymbol{q}, \dot{\boldsymbol{q}}) = \begin{bmatrix} 0 & 0 & m_1 d\dot{\theta}\cos\theta & 0 & 0 \\ 0 & 0 & m_1 d\dot{\theta}\sin\theta & 0 & 0 \\ 0 & 0 & 0 & 0 & 0 \\ 0 & 0 & 0 & 0 & 0 \\ 0 & 0 & 0 & 0 & 0 \end{bmatrix}, \quad (48)$$

$$\boldsymbol{B}(\boldsymbol{q}) = \begin{bmatrix} 0 & 0 \\ 0 & 0 \\ 0 & 0 \\ 1 & 0 \\ 0 & 1 \end{bmatrix}.$$

In the case considered here we have three constraint forces.

In order to calculate the constraint forces one can multiply both sides of the first equation from the set of equations (47) by $\sin\theta$, the second by $-\cos\theta$ and sum up the resulting equations allows to find the first Lagrange multiplier

$$\lambda_1 = m_1 \ddot{x}_c \sin\theta - m_1 \ddot{y}_c \cos\theta + m_1 d\ddot{\theta}. \quad (49)$$

Next we differentiate both sides of Eq. (1) with respect to time and multiply by m_1

$$m_1\ddot{x}_c\sin\theta - m_1\ddot{y}_c\cos\theta = -m_1\dot{\theta}\left(\dot{y}_c\sin\theta + \dot{x}_c\cos\theta\right) - m_1 d\ddot{\theta}. \tag{50}$$

Combining Eqs. (49) and (50) gives

$$\lambda_1 = -m_1\dot{\theta}\left(\dot{y}_c\sin\theta + \dot{x}_c\cos\theta\right). \tag{51}$$

which is an expression for the first Lagrange multiplier. Now using three first equations from the set given by Eq. (47), Eq. (49), and Eqs. (3), and (4) (the last two in a similar way as Eq. (1)) we can calculate next two constraint forces

$$\lambda_2 = \frac{1}{2R}\left(J_1 - m_0 d^2\right)\ddot{\theta} + \frac{1}{4}m_1\left(\dot{x}_c\dot{\theta}\sin\theta - \dot{y}_c\dot{\theta}\cos\theta - R\ddot{\theta} + r\ddot{\varphi}_r\right), \tag{52}$$

$$\lambda_3 = -\frac{1}{2R}\left(J_1 - m_0 d^2\right)\ddot{\theta} + \frac{1}{4}m_1\left(\dot{x}_c\dot{\theta}\sin\theta - \dot{y}_c\dot{\theta}\cos\theta + R\ddot{\theta} + r\ddot{\varphi}_r\right). \tag{53}$$

Vector of constraint forces describes reaction forces which is a vector of Coulomb friction forces. It is possible to calculate two components tangent and normal of reaction force acting at each wheel. Coulomb friction forces at each wheel can be calculated as follows

$$T_{Nr} = \sqrt{\left(\frac{\lambda_1}{2}\right)^2 + \lambda_2^2} = \sqrt{{T_{Or}}^2 + {T_{Pr}}^2}, \tag{54}$$

$$T_{Nl} = \sqrt{\left(\frac{\lambda_1}{2}\right)^2 + \lambda_3^2} = \sqrt{{T_{Ol}}^2 + {T_{Pl}}^2}, \tag{55}$$

where T_{Or} and T_{Ol} are components acting along the wheels while T_{Pr} and T_{Pl} are transverse components of the Coulomb friction for right and left wheel, respectively. These forces are contact forces at the contact point between the wheels and the plane. These forces projected on the axes of the base coordinate system $\mathbf{XY}$ are the reaction forces R_x, R_y and M_R which appear on the right hand side of Eq. (47) (in this case first three equations from the set given by Eq. (47)). These forces are visualized in Fig. (3). Load force exerted by the vehicle on the plane is given by $F_N = (m_0 + 2m_w)g$. Based on the above considerations one can calculate maximal longitudinal, T_{Omax}, and transverse, T_{Pmax}, forces which when exceeded result in longitudinal and transverse sliding of both wheels. Denoting by μ_N coefficient of the Coulomb friction force one can write the following relationships

$$T_{Nr} \leqslant \mu_N \tfrac{1}{2} F_N \quad \text{and} \quad T_{Nl} \leqslant \mu_N \tfrac{1}{2} F_N. \tag{56}$$

When the above inequalities are not satisfied the nonholonomic constraints given by Eq. (5) are not satisfied too.

For subsequent considerations we will consider a set of equations (47) with coordinates x_c, y_c, θ, φ_r, φ_l and their first and second derivatives. It would be more suitable to

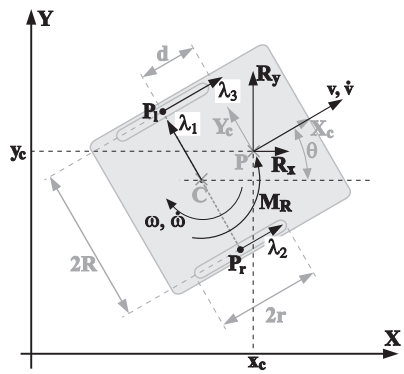

Figure 3. Reaction forces in $\mathbf{XY}$ base coordinate system

express the dynamic equations of motion in terms of internal velocities v and ω. In order to do that we differentiate Eq. (11) with respect to time. One can get

$$\ddot{\boldsymbol{q}} = \dot{\boldsymbol{S}}(\boldsymbol{q})\boldsymbol{\nu} + \boldsymbol{S}(\boldsymbol{q})\dot{\boldsymbol{\nu}}. \tag{57}$$

Next we substitute Eqs. (11) and (57) in Eq. (17) and multiply the resulting equation on the left hand side by matrix $\boldsymbol{S}^T(\boldsymbol{q})$. After some not complicated calculations we get

$$\bar{\boldsymbol{M}}(\boldsymbol{q})\dot{\boldsymbol{\nu}} + \bar{\boldsymbol{V}}_m(\boldsymbol{q},\dot{\boldsymbol{q}})\boldsymbol{\nu} + \bar{\boldsymbol{F}}(\boldsymbol{\nu}) + \bar{\boldsymbol{\tau}}_z = \bar{\boldsymbol{B}}(\boldsymbol{q})\boldsymbol{\tau}, \tag{58}$$

where $\bar{\boldsymbol{M}} = \boldsymbol{S}^T\boldsymbol{M}\boldsymbol{S}, \bar{\boldsymbol{V}}_m = \boldsymbol{S}^T[\boldsymbol{M}\dot{\boldsymbol{S}}+\boldsymbol{V}_m\boldsymbol{S}], \bar{\boldsymbol{F}} = \boldsymbol{S}^T\boldsymbol{F}, \bar{\boldsymbol{\tau}}_z = \boldsymbol{S}^T\boldsymbol{\tau}_z$ and $\bar{\boldsymbol{B}} = \boldsymbol{S}^T\boldsymbol{B}$. As before $\boldsymbol{\tau}$ is a set of two moments acting at the wheels, namely $[\tau_r\ \tau_l]^T$. Matrix $\bar{\boldsymbol{M}}(\boldsymbol{q})$ which appears in Eq. (58) is positive definite and matrix $\dot{\bar{\boldsymbol{M}}} - 2\bar{\boldsymbol{V}}_m$ is a skew symmetric matrix. In order to prove the last property we calculate the time derivative of matrix $\bar{\boldsymbol{M}}$, namely $\dot{\bar{\boldsymbol{M}}} = \dot{\boldsymbol{S}}^T\boldsymbol{M}\boldsymbol{S} + \boldsymbol{S}^T\dot{\boldsymbol{M}}\boldsymbol{S} + \boldsymbol{S}^T\boldsymbol{M}\dot{\boldsymbol{S}}$. Therefore we have

$$\dot{\bar{\boldsymbol{M}}} - 2\bar{\boldsymbol{V}}_m = \dot{\boldsymbol{S}}^T\boldsymbol{M}\boldsymbol{S} - (\dot{\boldsymbol{S}}^T\boldsymbol{M}\boldsymbol{S})^T + \boldsymbol{S}^T(\dot{\boldsymbol{M}} - 2\boldsymbol{V}_m)\boldsymbol{S}. \tag{59}$$

From the last equation it is clear that $\dot{\bar{\boldsymbol{M}}} - 2\bar{\boldsymbol{V}}_m$ is a skew symmetric matrix. Straightforward calculations show that in dynamic equations of motion given by (47)-(48) matrices $\bar{\boldsymbol{M}}$ and $\bar{\boldsymbol{V}}_m$ have the following form

$$\bar{\boldsymbol{M}} = \begin{bmatrix} m_0 + 2m_w + 2C_n\frac{1}{r^2} & 0 \\ 0 & J_0 + 2A_k + 2m_wR^2 + 2\frac{R^2}{r^2}C_n \end{bmatrix}, \quad \bar{\boldsymbol{V}}_m = \boldsymbol{0}. \tag{60}$$

In all calculation we have used matrix $\boldsymbol{S}_1(\boldsymbol{q})$ which follows directly from Eq. (13). Matrix $\bar{\boldsymbol{B}}$ is of the form $\bar{\boldsymbol{B}} = \begin{bmatrix} \frac{1}{r} & \frac{1}{r} \\ \frac{R}{r} & -\frac{R}{r} \end{bmatrix}$. Note that matrix $\bar{\boldsymbol{B}}$ is nonsingular.

Applying the same procedure to a set of equation (35)-(39) and using matrix $\boldsymbol{S}_2(\boldsymbol{q}_1)$ which follows from Eq. (14) it is easy to calculate that matrices $\bar{\boldsymbol{M}}_1$ and $\boldsymbol{V}_{m1}$ are exactly the same as matrix given by Eq. (60). This result is obvious since in both cases steering signals are linear and angular velocities of the vehicle.

Now we are in position to take into account electrical part of the actuators. It is assumed that both motors are DC motors. We denote by indices r and l right and left motor, respectively. Equations governing the right actuator can be written as follows

$$\tau_{sr} = k_{ir} i_r, \tag{61}$$

$$U_r = L_r \frac{di_r}{dt} + R_{ar} i_r + k_{er} \dot{\varphi}_r, \tag{62}$$

where τ_{sr} is the torque generated by the right motor. In Eq. (61) it is assumed that the current is proportional to the torque and constant coefficient which plays this role is denoted by k_{ir}. Equation (62) characterizes voltage equation of the armature which is described by inductance L_r and resistance R_{ar}, while k_{er} denotes counter electromotive force coefficient. Torques for both motors can be written in more compact form as

$$\boldsymbol{\tau}_s = \begin{bmatrix} \tau_{sr} \\ \tau_{sl} \end{bmatrix} = \begin{bmatrix} k_{ir} & 0 \\ 0 & k_{il} \end{bmatrix} \begin{bmatrix} i_r \\ i_l \end{bmatrix} = \boldsymbol{k}_i \boldsymbol{i} \tag{63}$$

and current-voltage equation has the following form

$$\begin{bmatrix} U_r \\ U_l \end{bmatrix} = \begin{bmatrix} L_r & 0 \\ 0 & L_l \end{bmatrix} \begin{bmatrix} \frac{di_r}{dt} \\ \frac{di_l}{dt} \end{bmatrix} + \begin{bmatrix} R_{ar} & 0 \\ 0 & R_{al} \end{bmatrix} \begin{bmatrix} i_r \\ i_l \end{bmatrix} + \begin{bmatrix} k_{er} & 0 \\ 0 & k_{el} \end{bmatrix} \begin{bmatrix} \dot{\varphi}_{sr} \\ \dot{\varphi}_{sl} \end{bmatrix}, \tag{64}$$

or in a matrix vector form

$$\boldsymbol{U} = \boldsymbol{L} \frac{d\boldsymbol{i}}{dt} + \boldsymbol{R}_a \boldsymbol{i} + \boldsymbol{k}_e \dot{\boldsymbol{\varphi}}_s. \tag{65}$$

Relationship between angular wheel velocities and internal velocities $\boldsymbol{\nu}$ is given by Eq. (12) which we rewrite as follows

$$\begin{bmatrix} \dot{\varphi}_r \\ \dot{\varphi}_l \end{bmatrix} = \begin{bmatrix} \frac{1}{r} & \frac{1}{2c} \\ \frac{1}{r} & -\frac{1}{2c} \end{bmatrix} \begin{bmatrix} v \\ \omega \end{bmatrix} = \boldsymbol{k}_v \boldsymbol{\nu} \tag{66}$$

Actuators are usually equipped with gears. Taking it into account one can write $\boldsymbol{\tau}_k = \boldsymbol{N}\boldsymbol{\tau}_s$ and $[\dot{\varphi}_{sr}\ \dot{\varphi}_{sl}]^T = \boldsymbol{N}^{-1}\dot{\boldsymbol{\varphi}}_s$. Then Eqs. (63) and (64) can be rewritten as follows

$$\boldsymbol{\tau}_k = \boldsymbol{N}\boldsymbol{k}_i \boldsymbol{i} \tag{67}$$

$$\boldsymbol{U} = \boldsymbol{L} \frac{d\boldsymbol{i}}{dt} + \boldsymbol{R}_a \boldsymbol{i} + \boldsymbol{k}_e \boldsymbol{N} \boldsymbol{k}_v \boldsymbol{\nu}, \tag{68}$$

where $\boldsymbol{N}$ is a diagonal matrix $\boldsymbol{N} = diag(n_r\ n_l)$, and gear ratios n_r and n_l are greater then 1. For subsequent analysis we assume that $\boldsymbol{\tau} = \boldsymbol{\tau}_k$.

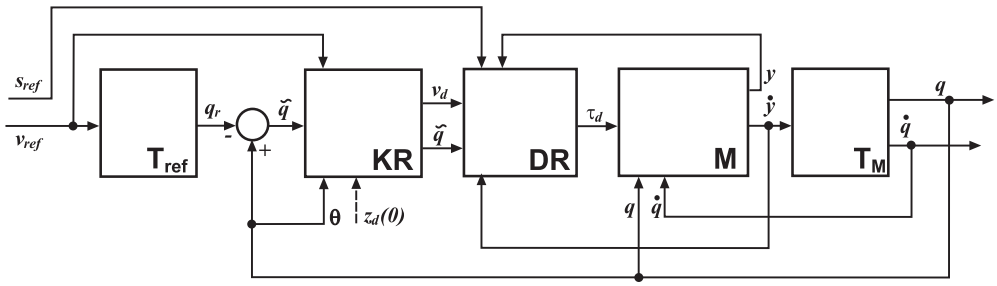

Figure 4. Model of control system for mobile robot

4. Backstepping procedure

In this section we present a backstepping algorithm which solves both trajectory tracking and set point control problems of a mobile robot considered in this paper. The overall systems consists of three loops, namely kinematic ($\mathbf{KR}$ in Fig. 4), dynamic ($\mathbf{DR}$ in Fig. 4), and servo (in block $\mathbf{M}$ in Fig. 4) which forms a backstepping scheme outlined in Fig. 4. In Fig. 4, $\mathbf{T}_{ref}$, denotes block trajectory generator, $\mathbf{T}_M$, is an executed trajectory and other signals which appear in Fig. 4 are described later in this section. $\boldsymbol{s}_{ref}$ and $\boldsymbol{v}_{ref}$ denote a vector of linear and angular reference path and velocities, respectively, while $\boldsymbol{y}$ and $\dot{\boldsymbol{y}}$ are executed path vector and its velocity.

The first loop solves a kinematic problem which is based on an idea of kinematic oscillator which was proposed by Dixon and coauthors [7]- [9]. The oscillator satisfies Brockett's conditions [5] for nonholonomic mobile robot considered here. We refer our considerations to a mobile robot presented in Fig. 1. Our control objective is to design a kinematic controller for both trajectory tracking and set-point control. First we introduce the following transformation for position and orientation tracking errors in the base coordinate system

$$\begin{bmatrix} w \\ z_1 \\ z_2 \end{bmatrix} = \begin{bmatrix} -\widetilde{\theta}\cos\theta + 2\sin\theta & -\widetilde{\theta}\sin\theta - 2\cos\theta & -2d \\ 0 & 0 & 1 \\ \cos\theta & \sin\theta & 0 \end{bmatrix} \begin{bmatrix} \widetilde{x} \\ \widetilde{y} \\ \widetilde{\theta} \end{bmatrix}, \tag{69}$$

or equivalently

$$\boldsymbol{w} = \boldsymbol{Z}\widetilde{\boldsymbol{x}}. \tag{70}$$

In the last equation $\widetilde{x}(t), \widetilde{y}(t), \widetilde{\theta}(t)$ denote difference between actual position and orientation $[x_c, y_c, \theta]$ of the center of mass of the vehicle and $[x_{rc}, y_{rc}, \theta_r]$ denote reference position and orientation expressed in the base coordinate system

$$\widetilde{\boldsymbol{x}} = \boldsymbol{q}_c - \boldsymbol{q}_{rc}, \quad \widetilde{x} = x_c - x_{rc}, \quad \widetilde{y} = y_c - y_{rc}, \quad \widetilde{\theta} = \theta - \theta_r. \tag{71}$$

Differentiating both sides of Eq. (69) and using (11) one can write the following differential equation for signals w, z_1 and z_2

$$\dot{w} = \boldsymbol{u}^T \boldsymbol{J}^T \boldsymbol{z} + f, \qquad \dot{\boldsymbol{z}} = \boldsymbol{u}, \tag{72}$$

where $\boldsymbol{J} \in \mathbb{R}^{2\times 2}$ is a skew symmetric matrix

$$\boldsymbol{J} = \begin{bmatrix} 0 & -1 \\ 1 & 0 \end{bmatrix}, \tag{73}$$

and function, $f \in \mathbb{R}$, has the form

$$f = 2(v_{r2} z_2 - v_{r1} \sin z_1 + d v_{r2} \cos z_1 + d v_{r2}), \tag{74}$$

where v_{r1} and v_{r2} are reference linear and angular velocities of the vehicle. Dixon and coauthors considered in their papers [7]- [9] the case $d = 0$. Here we extended their results to nonholonomic constraints assuming that internal coordinates are linear and angular velocities of the vehicle. Now we define an auxiliary variable $\boldsymbol{u}(t) = [u_1(t)\ u_2(t)]^T \in \mathbb{R}^2$ in terms of the position and orientation, velocities, and an auxiliary error signal $\widetilde{\boldsymbol{z}}(t) \in \mathbb{R}^2$ as the difference between the subsequently desired auxiliary signal $\boldsymbol{z}_d(t) \in \mathbb{R}^2$ and the transformed variable $\boldsymbol{z}(t)$, defined in (70), as follows

$$\widetilde{\boldsymbol{z}} = \boldsymbol{z}_d - \boldsymbol{z}. \tag{75}$$

Based on the kinematic equation given by Eq. (70), Dixon and coauthors designed the auxiliary signal $\boldsymbol{u}(t)$ as follows

$$\boldsymbol{u} = \boldsymbol{u}_a - k_2 \boldsymbol{z}, \tag{76}$$

where the control term $\boldsymbol{u}_a(t) \in \mathbb{R}^2$ is defined as

$$\boldsymbol{u}_a = \left(\frac{k_1 w + f}{{\delta_d}^2} \right) \boldsymbol{J} \boldsymbol{z}_d + \Omega_1 \boldsymbol{z}_d. \tag{77}$$

The auxiliary signal $\boldsymbol{z}_d(t)$ is defined by the following oscillator-like relationship

$$\dot{\boldsymbol{z}}_d = \frac{\dot{\delta}_d}{\delta_d} \boldsymbol{z}_d + \left(\frac{k_1 w + f}{{\delta_d}^2} + w\Omega_1 \right) \boldsymbol{J} \boldsymbol{z}_d, \tag{78}$$

with initial condition

$$\boldsymbol{z}_d^T(0) \boldsymbol{z}_d(0) = {\delta_d}^2(0), \tag{79}$$

and $\Omega_1 \in \mathbb{R}$ is defined as

$$\Omega_1 = k_2 + \frac{\dot{\delta}_d}{\delta_d} + w \left(\frac{k_1 w + f}{{\delta_d}^2} \right), \tag{80}$$

where

$$\delta_d = \alpha_0 e^{-\alpha_1 t} + \varepsilon_1. \tag{81}$$

All coefficients $k_1, k_2, \alpha_0, \alpha_1$ and $\varepsilon_1 \in \mathbb{R}$ are positive, constant control gains. Dixon and coauthors proved in a systematic manner the following theorem [7].

Theorem 1. *Provided the reference trajectory is selected to be bounded for all time $t \geqslant 0$, the kinematic control law given by Eqs. (70)-(81) ensures the position and orientation tracking errors defined in Eq. (69) are globally uniformly ultimately bounded in the case that*

$$|\widetilde{x}(t)|, |\widetilde{y}(t)|, |\widetilde{\theta}(t)| \leqslant \beta_0 e^{-\gamma_0 t} + \beta_1 \varepsilon_1, \tag{82}$$

where ε_1, which can be made arbitrary small, was defined in Eq. (81), and β_0, β_1 and $\gamma_0 \in \mathbb{R}$ are some positive constants.

Proof of the theorem in based on Lyapunov stability analysis and can be found in reference [7]. The stability analysis is carried out in terms of variables $w(t)$, $z_1(t)$, $z_2(t)$, however inverse transformation to one given in Eq. (69) leads to variables $\widetilde{x}$, $\widetilde{y}$,$\widetilde{\theta}$ according to the following equation

$$\begin{bmatrix} \widetilde{x} \\ \widetilde{y} \\ \widetilde{\theta} \end{bmatrix} = \begin{bmatrix} \frac{1}{2}\sin\theta & d\sin\theta & \frac{1}{2}\widetilde{\theta}\sin\theta + \cos\theta \\ -\frac{1}{2}\cos\theta & -d\cos\theta & -\frac{1}{2}\widetilde{\theta}\cos\theta + \sin\theta \\ 0 & 1 & 0 \end{bmatrix} \begin{bmatrix} w \\ z_1 \\ z_2 \end{bmatrix}. \tag{83}$$

Next step of the backstepping procedure incorporates dynamic equations of motion of the vehicle in the form of Eq. (58). First we rewrite a reference trajectory as

$$\boldsymbol{u} = \boldsymbol{T}^{-1}\boldsymbol{\nu} - \begin{bmatrix} v_{r2} \\ v_{r1}\cos\widetilde{\theta} + 2v_{r2}\sin\widetilde{\theta} \end{bmatrix}. \tag{84}$$

Last equation is merely a rearrangement of the second equation of Eq. (72). Based on Eq. (84) one can calculate a vector of actual velocities of the vehicle

$$\boldsymbol{\nu} = \boldsymbol{T}\boldsymbol{u} + \begin{bmatrix} v_{r1}\cos\widetilde{\theta} + v_{r2}(\widetilde{x}\sin\theta - \widetilde{y}\cos\theta) + 2v_{r2}\sin\widetilde{\theta} \\ v_{r2} \end{bmatrix}. \tag{85}$$

In Eqs. (84) and (85) matrix $\boldsymbol{T} \in \mathbb{R}^{2\times 2}$ has the following form

$$\boldsymbol{T} = \begin{bmatrix} (\widetilde{x}\sin\theta - \widetilde{y}\cos\theta) & 1 \\ 1 & 0 \end{bmatrix}. \tag{86}$$

In order to do that we rewrite Eq. (85) as follows

$$\boldsymbol{\nu} = \boldsymbol{T}\boldsymbol{u} + \boldsymbol{\Pi}_1, \tag{87}$$

where vector $\boldsymbol{\Pi}_1$ is defined clearly in Eq. (85). Differentiation of Eq. (87) with respect to time gives

$$\dot{\boldsymbol{\nu}} = \dot{\boldsymbol{T}}\boldsymbol{u} + \boldsymbol{T}\dot{\boldsymbol{u}} + \boldsymbol{\Pi}, \tag{88}$$

where vector $\mathbf{\Pi}^{2\times 1}$ has the following form

$$\mathbf{\Pi} = \begin{bmatrix} \dot{v}_{r1}\cos\widetilde{\theta} - v_{r1}\dot{\widetilde{\theta}}\sin\widetilde{\theta} + \dot{v}_{r2}(\widetilde{x}\sin\theta - \widetilde{y}\cos\theta) + \\ +v_{r2}(\widetilde{x}\dot{\theta}\cos\theta + \dot{\widetilde{x}}\sin\theta + \widetilde{y}\dot{\theta}\sin\theta - \dot{\widetilde{y}}\cos\theta) + 2\dot{v}_{r2}\sin\widetilde{\theta} + 2v_{r2}\dot{\widetilde{\theta}}\cos\widetilde{\theta} \\ \text{- - - - - - - - - - - -} \\ \dot{v}_{r2} \end{bmatrix}. \tag{89}$$

Substitution of Eqs. (87) and (88) in Eq. (58) results

$$\bar{\boldsymbol{M}}(\boldsymbol{q})\left[\dot{\boldsymbol{T}}\boldsymbol{u} + \boldsymbol{T}\dot{\boldsymbol{u}} + \mathbf{\Pi}\right] + \bar{\boldsymbol{V}}_m(\boldsymbol{q},\dot{\boldsymbol{q}})\left[\boldsymbol{T}\boldsymbol{u} + \mathbf{\Pi}_1\right] + \bar{\boldsymbol{F}}(\boldsymbol{\nu}) + \bar{\boldsymbol{\tau}}_z = \bar{\boldsymbol{B}}(\boldsymbol{q})\boldsymbol{\tau}. \tag{90}$$

Next we multiply Eq. (90) by $\boldsymbol{T}^T$ on the left hand side

$$\begin{gathered} \boldsymbol{T}^T\bar{\boldsymbol{M}}(\boldsymbol{q})\boldsymbol{T}\dot{\boldsymbol{u}} + \boldsymbol{T}^T\bar{\boldsymbol{M}}(\boldsymbol{q})\dot{\boldsymbol{T}}\boldsymbol{u} + \boldsymbol{T}^T\bar{\boldsymbol{M}}(\boldsymbol{q})\mathbf{\Pi} + \\ \boldsymbol{T}^T\bar{\boldsymbol{V}}_m(\boldsymbol{q},\dot{\boldsymbol{q}})\boldsymbol{T}\boldsymbol{u} + \boldsymbol{T}^T\bar{\boldsymbol{V}}_m(\boldsymbol{q},\dot{\boldsymbol{q}})\mathbf{\Pi}_1 + \boldsymbol{T}^T\bar{\boldsymbol{F}}(\boldsymbol{\nu}) + \boldsymbol{T}^T\bar{\boldsymbol{\tau}}_z = \boldsymbol{T}^T\bar{\boldsymbol{B}}(\boldsymbol{q})\boldsymbol{\tau}. \end{gathered} \tag{91}$$

Now we introduce the following idea of the control law which incorporates dynamic equations of motion of the vehicle. We assume that the control vector given in Eq. (76) is an input control signal to the system including dynamics of the vehicle. Now signal given in Eq. (76) is considered as the second step of the backstepping procedure [17]. We denote this signal as $\boldsymbol{u}_d \in \mathbb{R}^2$. Next we define the following error between the desired signal $\boldsymbol{u}_d$ and actual signal $\boldsymbol{u}$

$$\boldsymbol{\eta} = \boldsymbol{u}_d - \boldsymbol{u}. \tag{92}$$

Differentiation of the last equation results in

$$\dot{\boldsymbol{u}} = \dot{\boldsymbol{u}}_d - \dot{\boldsymbol{\eta}}. \tag{93}$$

Now we substitute Eqs. (92) and (93) into Eq. (91) which gives

$$\begin{gathered} \bar{\bar{\boldsymbol{M}}}(\boldsymbol{q})(\dot{\boldsymbol{u}}_d - \dot{\boldsymbol{\eta}}) + \boldsymbol{T}^T\bar{\boldsymbol{M}}(\boldsymbol{q})\dot{\boldsymbol{T}}(\boldsymbol{u}_d - \boldsymbol{\eta}) + \\ \boldsymbol{T}^T\bar{\boldsymbol{M}}(\boldsymbol{q})\mathbf{\Pi} + \boldsymbol{T}^T\bar{\boldsymbol{V}}_m(\boldsymbol{q},\dot{\boldsymbol{q}})\boldsymbol{T}(\boldsymbol{u}_d - \boldsymbol{\eta}) + \\ \boldsymbol{T}^T\bar{\boldsymbol{V}}_m(\boldsymbol{q},\dot{\boldsymbol{q}})\mathbf{\Pi}_1 + \boldsymbol{T}^T\bar{\boldsymbol{F}}(\boldsymbol{\nu}) + \boldsymbol{T}^T\bar{\boldsymbol{\tau}}_z = \boldsymbol{T}^T\bar{\boldsymbol{B}}(\boldsymbol{q})\boldsymbol{\tau}, \end{gathered} \tag{94}$$

where $\bar{\bar{\boldsymbol{M}}} = \boldsymbol{T}^T\bar{\boldsymbol{M}}(\boldsymbol{q})\boldsymbol{T}$. Note that matrix $\bar{\bar{\boldsymbol{M}}}$ is symmetric. Next we rewrite Eq. (94) in the following form

$$\bar{\bar{\boldsymbol{M}}}\dot{\boldsymbol{\eta}} = -\boldsymbol{R} - \boldsymbol{T}^T\bar{\boldsymbol{M}}(\boldsymbol{q})\dot{\boldsymbol{T}}\boldsymbol{\eta} - \boldsymbol{T}^T\bar{\boldsymbol{V}}_m(\boldsymbol{q},\dot{\boldsymbol{q}})\boldsymbol{T}\boldsymbol{\eta} - \boldsymbol{T}^T\bar{\boldsymbol{B}}(\boldsymbol{q})\boldsymbol{\tau}, \tag{95}$$

where

$$\begin{gathered} \boldsymbol{R} = -\bar{\bar{\boldsymbol{M}}}\dot{\boldsymbol{u}}_d - \boldsymbol{T}^T\bar{\boldsymbol{M}}(\boldsymbol{q})\boldsymbol{T}\boldsymbol{u}_d - \boldsymbol{T}^T\bar{\boldsymbol{M}}\mathbf{\Pi} + \\ -\boldsymbol{T}^T\bar{\boldsymbol{V}}_m(\boldsymbol{q},\dot{\boldsymbol{q}})\boldsymbol{T}\boldsymbol{u}_d - \boldsymbol{T}^T\bar{\boldsymbol{V}}_m\mathbf{\Pi}_1 - \boldsymbol{T}^T\bar{\boldsymbol{F}}(\boldsymbol{\nu}) - \boldsymbol{T}^T\bar{\boldsymbol{\tau}}_z. \end{gathered} \tag{96}$$

Since the matrix $\bar{\bar{\boldsymbol{M}}}$ is nonsingular one can write the following differential equation governing error $\boldsymbol{\eta}$

$$\dot{\boldsymbol{\eta}} = \left[\bar{\bar{\boldsymbol{M}}}\right]^{-1}\left[-\boldsymbol{R} - \boldsymbol{T}^T\bar{\boldsymbol{M}}(\boldsymbol{q})\dot{\boldsymbol{T}}\boldsymbol{\eta}\right] - \left[\bar{\bar{\boldsymbol{M}}}\right]^{-1}\left[\boldsymbol{T}^T\bar{\boldsymbol{V}}_m(\boldsymbol{q},\dot{\boldsymbol{q}})\boldsymbol{T}\boldsymbol{\eta} + \boldsymbol{T}^T\bar{\boldsymbol{B}}(\boldsymbol{q})\boldsymbol{\tau}\right]. \quad (97)$$

According to the assumption that the signal $\boldsymbol{u}_d$ is originated in the kinematic oscillator we can write

$$\boldsymbol{u}_d = \boldsymbol{u}_a - k_2\boldsymbol{z}, \quad (98)$$

and $\boldsymbol{u}_a$ is defined in Eq. (77). In order to continue the derivations we first formulate differential equations governing transformed errors w and $\widetilde{\boldsymbol{z}}$. Consider now the first equation in (72). Using Eq. (75) adding and subtracting $\boldsymbol{u}_a^T\boldsymbol{J}\boldsymbol{z}$ and substituting $\boldsymbol{u}$ from (92) gives the following results

$$\dot{w} = \boldsymbol{u}_a^T\boldsymbol{J}\widetilde{\boldsymbol{z}} + \boldsymbol{\eta}^T\boldsymbol{J}\boldsymbol{z} - \boldsymbol{u}_a^T\boldsymbol{J}\boldsymbol{z}_d + f. \quad (99)$$

where we use $\boldsymbol{J}^T = -\boldsymbol{J}$. In order to eliminate f in the last equation one can use Eq. (77) and substitution of it in the third component of Eq. (99), using $\boldsymbol{J}^T\boldsymbol{J} = \boldsymbol{I}_2$, gives

$$\dot{w} = -k_1 w + \boldsymbol{u}_a^T\boldsymbol{J}\widetilde{\boldsymbol{z}} + \boldsymbol{\eta}^T\boldsymbol{J}\boldsymbol{z}. \quad (100)$$

In order to obtain differential equation in terms of error $\widetilde{\boldsymbol{z}}$ we differentiate with respect to time Eq. (75) and use Eqs. (78), and Eq. (92) which results in

$$\dot{\widetilde{\boldsymbol{z}}} = \frac{\dot{\delta}_d}{\delta_d}\boldsymbol{z}_d + \left(\frac{k_1 w + f}{{\delta_d}^2} + w\Omega_1\right)\boldsymbol{J}\boldsymbol{z}_d + \boldsymbol{\eta} - \boldsymbol{u}_d. \quad (101)$$

We rearrange the last equation substituting Eq. (98) in Eq. (101)

$$\dot{\widetilde{\boldsymbol{z}}} = \frac{\dot{\delta}_d}{\delta_d}\boldsymbol{z}_d - \Omega_1\boldsymbol{z}_d + \boldsymbol{\eta} + k_2\boldsymbol{z} + w\Omega_1\boldsymbol{J}\boldsymbol{z}_d. \quad (102)$$

Using Eq. (80) in Eq. (102) and observing that $\boldsymbol{J}\boldsymbol{J} = -\boldsymbol{I}_2$ gives

$$\dot{\widetilde{\boldsymbol{z}}} = -k_2\widetilde{\boldsymbol{z}} + w\boldsymbol{J}\boldsymbol{u}_a + \boldsymbol{\eta}. \quad (103)$$

In order to prove the stability of the system consisting of model kinematics (see Eq. (69)) and dynamics (see Eq. (95)), which is the second step of the backstepping procedure, we propose to use the following Lyapunov function candidate

$$V = \frac{1}{2}w^2 + \frac{1}{2}\widetilde{\boldsymbol{z}}^T\widetilde{\boldsymbol{z}} + \frac{1}{2}\boldsymbol{\eta}^T\bar{\bar{\boldsymbol{M}}}\boldsymbol{\eta} + \frac{1}{2}a^2. \quad (104)$$

First two components represent energy of the transformed errors, the third component is a kinetic energy of the vehicle described in terms of input error, and finally the last term

describes a square of certain function which depends on time and will be defined later. Time derivative of the Lyapunov function has the following form

$$\dot{V} = w\dot{w} + \widetilde{\boldsymbol{z}}^T \dot{\widetilde{\boldsymbol{z}}} + \boldsymbol{\eta}^T \bar{\bar{\boldsymbol{M}}} \dot{\boldsymbol{\eta}} + \frac{1}{2} \boldsymbol{\eta}^T \frac{d}{dt} \left[\bar{\bar{\boldsymbol{M}}} \right] \boldsymbol{\eta} + a\dot{a}. \tag{105}$$

Substitution of Eqs. (100), (103) and (97) in Eq. (105) gives

$$\dot{V} = w[-k_1 w + \boldsymbol{u}_a^T \boldsymbol{J} \widetilde{\boldsymbol{z}} + \boldsymbol{\eta}^T \boldsymbol{J} \boldsymbol{z}] + \widetilde{\boldsymbol{z}}^T [-k_2 \widetilde{\boldsymbol{z}} + w \boldsymbol{J} \boldsymbol{u}_a + \boldsymbol{\eta}] + a\dot{a} + \frac{1}{2} \boldsymbol{\eta}^T \frac{d}{dt} \left[\bar{\bar{\boldsymbol{M}}} \right] \boldsymbol{\eta} +$$

$$\boldsymbol{\eta}^T \bar{\bar{\boldsymbol{M}}} \left[\bar{\bar{\boldsymbol{M}}} \right]^{-1} \left[-\boldsymbol{R} - \boldsymbol{T}^T \bar{\boldsymbol{M}}(\boldsymbol{q}) \dot{\boldsymbol{T}} \boldsymbol{\eta} \right] - \tag{106}$$

$$\boldsymbol{\eta}^T \bar{\bar{\boldsymbol{M}}} \left[\bar{\bar{\boldsymbol{M}}} \right]^{-1} \left[\boldsymbol{T}^T \bar{\boldsymbol{V}}_m(\boldsymbol{q}, \dot{\boldsymbol{q}}) \boldsymbol{T} \boldsymbol{\eta} + \boldsymbol{T}^T \bar{\boldsymbol{B}}(\boldsymbol{q}) \boldsymbol{\tau} \right].$$

It is easy to prove that matrix $\frac{1}{2} \frac{d}{dt} \left[\bar{\bar{\boldsymbol{M}}} \right] - \boldsymbol{T}^T \bar{\boldsymbol{M}} \dot{\boldsymbol{T}} - \boldsymbol{T}^T \bar{\boldsymbol{V}}_m \boldsymbol{T}$ is a skew symmetric matrix. Therefore one can write $\dot{V}$ as follows

$$\dot{V} = -w k_1 w + w \boldsymbol{\eta}^T \boldsymbol{J} \boldsymbol{z} - \widetilde{\boldsymbol{z}}^T k_2 \widetilde{\boldsymbol{z}} + \widetilde{\boldsymbol{z}}^T \boldsymbol{\eta} + \boldsymbol{\eta}^T \left[-\boldsymbol{R} - \boldsymbol{T}^T \bar{\boldsymbol{B}}(\boldsymbol{q}) \boldsymbol{\tau} \right] + a\dot{a}. \tag{107}$$

In order to reduce furthermore the last expression one can use the following relationship $\boldsymbol{R}_1 = \boldsymbol{R} - \boldsymbol{J} \boldsymbol{z} w - \widetilde{\boldsymbol{z}}$ which gives

$$\dot{V} = -k_1 w^2 - \widetilde{\boldsymbol{z}}^T k_2 \widetilde{\boldsymbol{z}} + \boldsymbol{\eta}^T \left[-\boldsymbol{R}_1 \right] + a\dot{a} - \boldsymbol{\eta}^T \boldsymbol{T}^T \bar{\boldsymbol{B}}(\boldsymbol{q}) \boldsymbol{\tau}. \tag{108}$$

Now we propose the following control law at the dynamic level

$$\boldsymbol{\tau} = \left[\boldsymbol{T}^T \bar{\boldsymbol{B}}(\boldsymbol{q}) \right]^{-1} \boldsymbol{\eta}. \tag{109}$$

In the case considered here matrix which appears in the last equation is nonsingular. Using matrix which is present in Eq. (32) (which stands for matrix $\bar{\boldsymbol{B}}(\boldsymbol{q})$) and Eq. (86) it is easy to calculate that

$$\boldsymbol{T}^T \bar{\boldsymbol{B}}(\boldsymbol{q}) = \frac{1}{r} \begin{bmatrix} \widetilde{x} \sin\theta - \widetilde{y} \cos\theta + R & \widetilde{x} \sin\theta - \widetilde{y} \cos\theta - R \\ 1 & 1 \end{bmatrix}. \tag{110}$$

Note that $\det \left[\boldsymbol{T}^T \bar{\boldsymbol{B}}(\boldsymbol{q}) \right] = \frac{2R}{r}$ therefore the last matrix is nonsingular. Substituting control law given in Eq. (109) in Eq. (108) gives

$$\dot{V} = -k_1 w^2 - \widetilde{\boldsymbol{z}}^T k_2 \widetilde{\boldsymbol{z}} - \boldsymbol{\eta}^T \boldsymbol{\eta} + \boldsymbol{\eta}^T [-\boldsymbol{R}_1] + a\dot{a}. \tag{111}$$

In order to reduce the last equation we assume that (this reduction will be discussed later in this paper)

$$a\dot{a} = \boldsymbol{\eta}^T \boldsymbol{R}_1, \tag{112}$$

which allows to rewrite the time derivative of the Lyapunov function as follows

$$\dot{V} = -k_1 w^2 - \tilde{\boldsymbol{z}}^T k_2 \tilde{\boldsymbol{z}} - \boldsymbol{\eta}^T \boldsymbol{\eta}. \tag{113}$$

Now, at the third step of the backstepping procedure, we include the torques acting at the motor level, which is the last level of control and at the same time the third step of the backstepping procedure [17]. Intuitively we define the following Lyapunov function candidate

$$V_1 = \frac{1}{2} w^2 + \frac{1}{2} \tilde{\boldsymbol{z}}^T \tilde{\boldsymbol{z}} + \frac{1}{2} \boldsymbol{\eta}^T \bar{\bar{\boldsymbol{M}}} \boldsymbol{\eta} + \frac{1}{2} a^2 + \frac{1}{2} (\boldsymbol{\tau}_d - \boldsymbol{\tau})^T (\boldsymbol{\tau}_d - \boldsymbol{\tau}) = V + \frac{1}{2} (\boldsymbol{\tau}_d - \boldsymbol{\tau})^T (\boldsymbol{\tau}_d - \boldsymbol{\tau}), \tag{114}$$

where we have made use of Eq. (104), $\boldsymbol{\tau}_d$ is a vector of reference torques and $\boldsymbol{\tau}$ denotes a vector of actual torques. The time derivative of the Lyapunov function candidate, V_1, assuming that the differential equation (112) is satisfied, has the following form

$$\dot{V}_1 = -k_1 w^2 - \tilde{\boldsymbol{z}}^T k_2 \tilde{\boldsymbol{z}} - \boldsymbol{\eta}^T \boldsymbol{T}^T \bar{\boldsymbol{B}}(\boldsymbol{q}) \boldsymbol{\tau} + (\boldsymbol{\tau}_d - \boldsymbol{\tau})^T (\dot{\boldsymbol{\tau}}_d - \dot{\boldsymbol{\tau}}). \tag{115}$$

Now we consider the last term which appears in Eq. (115). Time differentiation of Eq. (67) gives

$$\frac{d\boldsymbol{\tau}_k}{dt} = \boldsymbol{N} \boldsymbol{k}_i \frac{d\boldsymbol{i}}{dt}. \tag{116}$$

Recall assumption that $\boldsymbol{\tau} = \boldsymbol{\tau}_k$. Substitution of Eq. (116) in Eq. (68) leads to

$$\boldsymbol{L} [\boldsymbol{N} \boldsymbol{k}_i]^{-1} \frac{d\boldsymbol{\tau}}{dt} = \boldsymbol{U} - \boldsymbol{H}(\boldsymbol{i}, \boldsymbol{\nu}), \tag{117}$$

where

$$\boldsymbol{H}(\boldsymbol{i}, \boldsymbol{\nu}) = \boldsymbol{R}_a \boldsymbol{i} + \boldsymbol{k}_e \boldsymbol{N} \boldsymbol{k}_\nu \boldsymbol{\nu}. \tag{118}$$

Notice that $\boldsymbol{\nu}$ is a vector of linear an angular velocities of the centre of mass of the vehicle. Now we propose the following control law at the voltage level

$$\boldsymbol{U} = \boldsymbol{L} [\boldsymbol{N} \boldsymbol{k_i}]^{-1} \frac{d\boldsymbol{\tau_d}}{dt} + \boldsymbol{H}(\boldsymbol{i}, \boldsymbol{v}) + \boldsymbol{L} [\boldsymbol{N} \boldsymbol{k}_i]^{-1} \boldsymbol{k}_{\boldsymbol{\tau}} (\boldsymbol{\tau_d} - \boldsymbol{\tau}) + \boldsymbol{L} [\boldsymbol{N} \boldsymbol{k_i}]^{-1} [\boldsymbol{\eta}^T \boldsymbol{T}^T \bar{\boldsymbol{B}}(\boldsymbol{q})]^T, \tag{119}$$

where $\boldsymbol{k}_\tau$ is a positive definite diagonal matrix. Substitution of Eq. (119) in Eq. (117) gives the following result

$$\frac{d\boldsymbol{\tau_d}}{dt} - \frac{d\boldsymbol{\tau}}{dt} = -\boldsymbol{k}_{\boldsymbol{\tau}} (\boldsymbol{\tau}_d - \boldsymbol{\tau}) - \left[\boldsymbol{\eta}^T \boldsymbol{T}^T \bar{\boldsymbol{B}}(\boldsymbol{q}) \right]^T. \tag{120}$$

Making use of Eq. (120) the time derivative $\dot{V}_1$ takes the following form

$$\dot{V}_1 = -k_1 w^2 - \tilde{\boldsymbol{z}}^T k_2 \tilde{\boldsymbol{z}} - \boldsymbol{\eta}^T \boldsymbol{T}^T \bar{\boldsymbol{B}}(\boldsymbol{q}_1) \boldsymbol{\tau} + (\boldsymbol{\tau}_d - \boldsymbol{\tau})^T \left[-\boldsymbol{k}_\tau (\boldsymbol{\tau}_d - \boldsymbol{\tau}) - \left(\boldsymbol{\eta}^T \boldsymbol{T}^T \bar{\boldsymbol{B}}(\boldsymbol{q}) \right)^T \right]. \tag{121}$$

We rewrite the above equation as follows

$$\begin{aligned}\dot{V}_1 = -k_1 w^2 - \widetilde{\boldsymbol{z}}^T k_2 \widetilde{\boldsymbol{z}} - \boldsymbol{\eta}^T \boldsymbol{T}^T \bar{\boldsymbol{B}} \boldsymbol{\tau} - (\boldsymbol{\tau}_d - \boldsymbol{\tau})^T \boldsymbol{k}_\tau (\boldsymbol{\tau}_d - \boldsymbol{\tau}) + \\ -\boldsymbol{\tau}_d^T \left(\boldsymbol{\eta}^T \boldsymbol{T}^T \bar{\boldsymbol{B}}\right)^T + \boldsymbol{\tau}^T \left(\boldsymbol{\eta}^T \boldsymbol{T}^T \bar{\boldsymbol{B}}\right)^T .\end{aligned} \tag{122}$$

Now we propose the following reference torque vector

$$\boldsymbol{\tau}_d = [\boldsymbol{T}^T \bar{\boldsymbol{B}}]^{-1} \boldsymbol{\eta}. \tag{123}$$

This construction is consistent with the backstepping procedure [17]. Recall that matrix $\boldsymbol{T}^T \bar{\boldsymbol{B}}(\boldsymbol{q})$ is defined correctly since it is nonsingular. Calculating transpose of Eq. (123) gives

$$\boldsymbol{\tau}_d^T = \boldsymbol{\eta}^T \left[\boldsymbol{T}^T \bar{\boldsymbol{B}}\right]^{-T} \tag{124}$$

Substituting the last equation in Eq. (122) leads to

$$\begin{aligned}\dot{V}_1 = -k_1 w^2 - \widetilde{\boldsymbol{z}}^T k_2 \widetilde{\boldsymbol{z}} - \boldsymbol{\eta}^T \boldsymbol{T}^T \bar{\boldsymbol{B}}(\boldsymbol{q}) \boldsymbol{\tau} - (\boldsymbol{\tau}_d - \boldsymbol{\tau})^T \boldsymbol{k}_\tau (\boldsymbol{\tau}_d - \boldsymbol{\tau}) + \\ -\boldsymbol{\eta}^T \underbrace{\left(\boldsymbol{T}^T \bar{\boldsymbol{B}}\right)^{-T} \left(\boldsymbol{T}^T \bar{\boldsymbol{B}}\right)^T}_{\boldsymbol{I}} \boldsymbol{\eta} + \boldsymbol{\tau}^T \left(\boldsymbol{\eta}^T \boldsymbol{T}^T \bar{\boldsymbol{B}}\right)^T .\end{aligned} \tag{125}$$

Now taking into account the following identity $\boldsymbol{\tau}^T \left(\boldsymbol{\eta}^T \boldsymbol{T}^T \bar{\boldsymbol{B}}\right) = \left[\left(\boldsymbol{\eta}^T \boldsymbol{T}^T \bar{\boldsymbol{B}}\right)^T \boldsymbol{\tau}\right]^T$ we get the following form of the time derivative of the Lyapunov function candidate

$$\dot{V}_1 = -k_1 w^2 - \widetilde{\boldsymbol{z}}^T k_2 \widetilde{\boldsymbol{z}} - \boldsymbol{\eta}^T \boldsymbol{\eta} - (\boldsymbol{\tau}_d - \boldsymbol{\tau})^T \boldsymbol{k}_\tau (\boldsymbol{\tau}_d - \boldsymbol{\tau}). \tag{126}$$

Note the Eq. (120) describes the differential equation governing torque error. In order to implement control law in Eq. (119) one has to substitute time derivative of the reference torques given by Eq. (124). For subsequent analysis we denote $\boldsymbol{\tau}_m = \boldsymbol{\tau}_d - \boldsymbol{\tau}$. Note that $\dot{V}_1$ is negative for all signals $w \neq 0, \widetilde{\boldsymbol{z}} \neq \boldsymbol{0}, \boldsymbol{\eta} \neq \boldsymbol{0}$ and $\boldsymbol{\tau}_m \neq \boldsymbol{0}$, and equal zero otherwise. Summarizing the above considerations we can propose the following theorem.

Theorem 2. *Assuming that the reference trajectory x_{rc}, y_{rc}, θ_r and its time derivatives are bounded signals for all $t \geqslant 0$ the dynamic control law given by Eqs. (75)-(81), (109), and (119) ensures the position and orientation tracking errors defined in Eq. (71) are globally uniformly ultimately bounded (to a neighborhood about zero that can be made arbitrary small) stability of the mobile vehicle described by kinematical, dynamical and drive system equations under the condition that certain integrals (given in Eq. (145) are bounded.*

PROOF. Note that the proof described above is based on backstepping procedure (all signals considered in the system are continuous).

Since the time derivative of the Lyapunov function candidate given by Eq. (126) is negative or zero and V_1 is lower bounded (by zero) and one can use Barbalat's Lemma (notice that $V_1(t)$ does not contain function $a(t)$) to show that V_1 tends to zero as $t \to \infty$

and therefore remains bounded for $t \in [0, \infty]$. Taking Eq. (126) denote by W the following function

$$W = k_1 \|w\|^2 + k_2 \|\widetilde{\boldsymbol{z}}\|^2 + \|\boldsymbol{\eta}\|^2 + k_{\tau min} \|\boldsymbol{\tau}_d - \boldsymbol{\tau}\|^2 \tag{127}$$

where $k_{\tau min}$ denotes the smallest value of the diagonal elements of matrix $\boldsymbol{k}_\tau$. Then we can write

$$\dot{V}_1 \leqslant -W. \tag{128}$$

Integrating both sides of Eq. (128) gives

$$\begin{aligned} 0 \leqslant \int_0^t W(\tau) d\tau \leqslant V_1 \left(0, w(0), \widetilde{\boldsymbol{z}}(0), \boldsymbol{\eta}(0), \boldsymbol{\tau}_d(0) - \boldsymbol{\tau}(0), a(0)\right) - \\ - V_1 \left(t, w(t), \widetilde{\boldsymbol{z}}(t), \boldsymbol{\eta}(t), \boldsymbol{\tau}_d(t) - \boldsymbol{\tau}(t), a(t)\right) \leqslant \\ V_1 \left(0, w(0), \widetilde{\boldsymbol{z}}(0), \boldsymbol{\eta}(0), \boldsymbol{\tau}_d(0) - \boldsymbol{\tau}(0), a(0)\right) \end{aligned} \tag{129}$$

because $V_1 \left(0, w(0), \widetilde{\boldsymbol{z}}(0), \boldsymbol{\eta}(0), \boldsymbol{\tau}_d(0) - \boldsymbol{\tau}(0), a(0)\right) \geqslant 0$. Therefore we can conclude that

$$\lim_{t \to \infty} \int_0^t W(\tau) d\tau < \infty \tag{130}$$

and Eq. (129) implies that $w(t)$, $\widetilde{\boldsymbol{z}}(t)$, $\boldsymbol{\eta}(t)$, $\boldsymbol{\tau}_d(t) - \boldsymbol{\tau}(t)$ are bounded signals for all $t \geqslant 0$. In order to be able to use Barbalat's Lemma [17] we have to prove that $\dot{V}_1$ is uniformly continuous in time. We recall here that it is sufficient to show that $\ddot{V}_1$ is bounded. We calculate the second time derivative of the Lyapunov function

$$\ddot{V}_1 = -2k_1 w\dot{w} - 2\widetilde{\boldsymbol{z}}^T k_2 \dot{\widetilde{\boldsymbol{z}}} - 2\boldsymbol{\eta}^T \dot{\boldsymbol{\eta}} - 2\left(\boldsymbol{\tau}_d - \boldsymbol{\tau}\right)^T \boldsymbol{k}_\tau \left(\dot{\boldsymbol{\tau}}_d - \dot{\boldsymbol{\tau}}\right). \tag{131}$$

Using Eqs. (100), (103), (95) and (120) the last equation has the following form

$$\begin{aligned} \ddot{V}_1 = -2k_1 w \left(-k_1 w + \boldsymbol{u}_a^T \boldsymbol{J} \widetilde{\boldsymbol{z}} + \boldsymbol{\eta}^T \boldsymbol{J} \widetilde{\boldsymbol{z}}\right) - 2\widetilde{\boldsymbol{z}} k_2 \left(-k_2 \widetilde{\boldsymbol{z}} + w \boldsymbol{J} \boldsymbol{u}_a + \boldsymbol{\eta}\right) + \\ -2\boldsymbol{\eta}^T \left[\bar{\bar{\boldsymbol{M}}}^{-1} \left(\boldsymbol{R} - \boldsymbol{T}^T \bar{\boldsymbol{M}} \dot{\boldsymbol{T}} \boldsymbol{\eta} - \boldsymbol{T}^T \bar{\boldsymbol{V}}_m \boldsymbol{T} \boldsymbol{\eta} - \boldsymbol{T}^T \bar{\boldsymbol{B}} \boldsymbol{\tau}\right)\right] + \\ -2(\boldsymbol{\tau}_d - \boldsymbol{\tau})^T \boldsymbol{k}_\tau \left[-\boldsymbol{k}_\tau (\boldsymbol{\tau}_d - \boldsymbol{\tau}) - \left(\boldsymbol{\eta}^T \boldsymbol{T}^T \bar{\boldsymbol{B}}\right)^T\right] = \\ = 2k_1^2 w^2 + 2\widetilde{\boldsymbol{z}}^T k_2^2 \widetilde{\boldsymbol{z}} + 2(\boldsymbol{\tau}_d - \boldsymbol{\tau})^T \boldsymbol{k}_\tau^2 (\boldsymbol{\tau}_d - \boldsymbol{\tau}) + 2\boldsymbol{\eta}^T \boldsymbol{\eta} + \\ -2\boldsymbol{\eta}^T \left[\bar{\bar{\boldsymbol{M}}}^{-1} \left(\boldsymbol{R} - \boldsymbol{T}^T \bar{\boldsymbol{M}} \dot{\boldsymbol{T}} \boldsymbol{\eta} - \boldsymbol{T}^T \bar{\boldsymbol{V}}_m \boldsymbol{T} \boldsymbol{\eta} - \boldsymbol{T}^T \bar{\boldsymbol{B}} \boldsymbol{\tau}\right)\right] + \\ -2\boldsymbol{\tau}^T \boldsymbol{k}_\tau \left(\boldsymbol{\eta}^T \boldsymbol{T}^T \bar{\boldsymbol{B}}\right)^T - 2k_1 w \left(\boldsymbol{u}_a^T \boldsymbol{J} \widetilde{\boldsymbol{z}} + \boldsymbol{\eta}^T \boldsymbol{J} \widetilde{\boldsymbol{z}}\right) - 2\widetilde{\boldsymbol{z}} k_2 \left(w \boldsymbol{J} \boldsymbol{u}_a + \boldsymbol{\eta}\right), \end{aligned} \tag{132}$$

where we have assumed that $\boldsymbol{k}_\tau$ is diagonal positive definite matrix. We have to prove that all terms which appear on the right hand side of Eq. (132) are bounded. Actually all signals belong to $\mathbb{L}_\infty$. First as it was mentioned above $w(t)$, $\widetilde{\boldsymbol{z}}(t)$, $\boldsymbol{\eta}(t)$, $\boldsymbol{\tau}_d(t) - \boldsymbol{\tau}(t) \in \mathbb{L}_\infty$ and therefore these signals are bounded. From Eqs. (75) and (79) and the fact that $\widetilde{\boldsymbol{z}}(t)$, $\delta_d(t) \in \mathbb{L}_\infty$ we can conclude that $\boldsymbol{z}(t)$ and $\boldsymbol{z}_d(t) \in \mathbb{L}_\infty$. From Eqs. (77) to (80) and the time derivative of (75), (92), (98), (100), (103) we can easily show that $\boldsymbol{u}_d(t)$, $\boldsymbol{u}_a(t)$, $\dot{\boldsymbol{z}}_d(t)$, $\dot{\widetilde{\boldsymbol{z}}}(t)$, $\dot{\boldsymbol{z}}(t)$, $\dot{w}(t)$, $\Omega_1(t)$ and $a(t)$ are bounded and belong to $\mathbb{L}_\infty$.

Furthermore from Eqs. (71) and (83) and the fact that $w(t)$, $\boldsymbol{z}(t)$,$\widetilde{\theta}(t) \in \mathbb{L}_\infty$ we can conclude that $\widetilde{x}(t)$, $\widetilde{y}(t)$, $x_c(t)$, $y_c(t) \in \mathbb{L}_\infty$.

Making use of Eq. (84), the assumption that the reference trajectory is differentiable, and the fact that $\theta(t)$, $\boldsymbol{u}(t)$, $\widetilde{x}$, $\widetilde{y} \in \mathbb{L}_\infty$, we can show that $\boldsymbol{\nu} \in \mathbb{L}_\infty$. Therefore using Eq. (14) it follows immediately that $\dot{\theta}(t)$, $\dot{x}_c(t)$, $\dot{y}_c(t) \in \mathbb{L}_\infty$. Using Eq. (123) it is easy to show that $\boldsymbol{\tau}_d$ is bounded and therefore $\boldsymbol{\tau}$ i bounded too. Clearly from Eq. (120) it follows that $\frac{d\boldsymbol{\tau}_d}{dt} - \frac{d\boldsymbol{\tau}}{dt}$ is bounded. From Eq. (95) it results that $\dot{\boldsymbol{\eta}}$ is bounded, therefore Eq. (123) results that $\frac{d\boldsymbol{\tau}_d}{dt}$ is bounded, and finally, from Eq. (120) one can deduce that $\frac{d\boldsymbol{\tau}}{dt}$ is bounded too. Boundness of $\bar{\bar{\boldsymbol{M}}}^{-1}$ follows from the following inequalities [9]

$$m_1\|\boldsymbol{\xi}\|^2 \leqslant \boldsymbol{\xi}^T \bar{\bar{\boldsymbol{M}}}^{-1}\boldsymbol{\xi} \leqslant m_2(\boldsymbol{z}, w)\|\boldsymbol{\xi}\|^2, \qquad \forall \boldsymbol{\xi} \in \mathbb{R}^2. \tag{133}$$

where m_1 is a known positive constant, $m_2(\boldsymbol{z}, w) \in \mathbb{R}^1$ is a known positive bounding function which is assumed to be bounded provided its arguments are bounded, and $\|\cdot\|$ stands for standard Euclidean norm. Since $\bar{\bar{\boldsymbol{M}}}$ is symmetric and positive definite, we can use (133) to show that the inverse of $\bar{\bar{\boldsymbol{M}}}$ satisfies the following inequality

$$\tfrac{1}{m_2(\boldsymbol{z},w)}\|\boldsymbol{\xi}\|^2 \leqslant \boldsymbol{\xi}^T \bar{\bar{\boldsymbol{M}}}^{-1}\boldsymbol{\xi} \leqslant \tfrac{1}{m_1}\|\boldsymbol{\xi}\|^2, \qquad \forall \boldsymbol{\xi} \in \mathbb{R}^2. \tag{134}$$

Taking time derivative of Eq. (98) after some tedious calculations one can show that$\dot{\boldsymbol{u}}_d$ is also bounded (see details in [9]). Therefore matrix $\boldsymbol{R}$ which appears in Eq. (132) which is given by Eq. (96) is bounded too. Finally, using standard signal chasing arguments we can conclude that all remaining signals in the control and the system remain bounded during closed-loop operation. By making use of Barbalat's Lemma we can conclude that all signals $w(t)$, $\widetilde{\boldsymbol{z}}(t)$, $\boldsymbol{\eta}(t)$ and $\boldsymbol{\tau}_d(t) - \boldsymbol{\tau}(t)$ tend asymptotically to zero. The same conclusion can be developed by making use of La Salle-Yoshizawa theorem [17] and [18]. Now taking into account Eq. (75) we can conclude that $\widetilde{\boldsymbol{z}}$ tends to $\boldsymbol{z}_d$ asymptotically. Therefore we get

$$\|\boldsymbol{z}\| \leqslant \|\boldsymbol{z}_d\| \leqslant \alpha_0 e^{-\alpha_1 t} + \varepsilon_1. \tag{135}$$

Now using Eq. (83) we conclude that $|\widetilde{x}(t)|$, $|\widetilde{y}(t)|$ and $|\widetilde{\theta}(t)|$ are globally uniformly ultimately bounded signals.

Now we go back to the discussion concerning definition of function $a(t)$. We rewrite Eq. (112) in the following form

$$a(t)\dot{a}(t) = \boldsymbol{\eta}^T(\boldsymbol{R} - \boldsymbol{J}\boldsymbol{z}w - \widetilde{\boldsymbol{z}}). \tag{136}$$

Recall that $\boldsymbol{R}$ can be calculated based on Eq. (95), namely

$$\boldsymbol{R} = -\bar{\bar{\boldsymbol{M}}}\dot{\boldsymbol{\eta}} - \boldsymbol{T}^T\bar{\boldsymbol{M}}\dot{\boldsymbol{T}}\boldsymbol{\eta} - \boldsymbol{T}^T\bar{\boldsymbol{V}}_m\boldsymbol{T}\boldsymbol{\eta} - \boldsymbol{T}^T\bar{\boldsymbol{B}}\boldsymbol{\tau}. \tag{137}$$

The control law at the dynamic level is calculated based on Eq. (109). Now we evaluate a scalar product $\boldsymbol{\eta}^T\boldsymbol{R}$ as follows

$$\boldsymbol{\eta}^T\boldsymbol{R} = \boldsymbol{\eta}^T\left[-\bar{\bar{\boldsymbol{M}}}\dot{\boldsymbol{\eta}} - \boldsymbol{T}^T\bar{\boldsymbol{M}}\dot{\boldsymbol{T}}\boldsymbol{\eta} - \boldsymbol{T}^T\bar{\boldsymbol{V}}_m\boldsymbol{T}\boldsymbol{\eta} - \boldsymbol{\eta}\right], \tag{138}$$

where we have made use of Eq. (109). Next recall that $\frac{1}{2}\frac{d}{dt}\bar{\bar{\boldsymbol{M}}} - \boldsymbol{T}^T\bar{\boldsymbol{M}}\dot{\boldsymbol{T}} - \boldsymbol{T}^T\bar{\boldsymbol{V}}_m\boldsymbol{T}$ is a skew symmetric matrix. As a consequence one can rewrite Eq. (138) as follows

$$\begin{gathered}\boldsymbol{\eta}^T\boldsymbol{R} = \boldsymbol{\eta}^T\left[-\bar{\bar{\boldsymbol{M}}}\dot{\boldsymbol{\eta}} - \boldsymbol{T}^T\bar{\boldsymbol{M}}\dot{\boldsymbol{T}}\boldsymbol{\eta} - \boldsymbol{T}^T\bar{\boldsymbol{V}}_m\boldsymbol{T}\boldsymbol{\eta} - \boldsymbol{\eta} + \tfrac{1}{2}\tfrac{d}{dt}\left(\bar{\bar{\boldsymbol{M}}}\right)\boldsymbol{\eta} - \tfrac{1}{2}\tfrac{d}{dt}\left(\bar{\bar{\boldsymbol{M}}}\right)\boldsymbol{\eta}\right] = \\ \boldsymbol{\eta}^T\left[-\bar{\bar{\boldsymbol{M}}}\dot{\boldsymbol{\eta}} - \boldsymbol{\eta} - \tfrac{1}{2}\tfrac{d}{dt}\left(\bar{\bar{\boldsymbol{M}}}\right)\boldsymbol{\eta}\right].\end{gathered} \tag{139}$$

Now we calculate the following time derivative of the kinetic energy

$$\frac{1}{2}\frac{d}{dt}\left[\boldsymbol{\eta}^T\bar{\bar{\boldsymbol{M}}}\boldsymbol{\eta}\right] = \frac{1}{2}\boldsymbol{\eta}^T\frac{d}{dt}\left[\bar{\bar{\boldsymbol{M}}}\right]\boldsymbol{\eta} + \boldsymbol{\eta}^T\bar{\bar{\boldsymbol{M}}}\dot{\boldsymbol{\eta}} \tag{140}$$

and substitute in Eq. (139)

$$\boldsymbol{\eta}^T\boldsymbol{R} = -\frac{1}{2}\frac{d}{dt}\left[\boldsymbol{\eta}^T\bar{\bar{\boldsymbol{M}}}\boldsymbol{\eta}\right] - \boldsymbol{\eta}^T\boldsymbol{\eta}. \tag{141}$$

On the other hand by making use of Eq. (141), Eq. (136) can be rewritten in the following form

$$\frac{d}{dt}a^2(t) = 2\dot{a}(t)a(t) = 2\left[-\frac{1}{2}\frac{d}{dt}\left(\boldsymbol{\eta}^T\bar{\bar{\boldsymbol{M}}}\boldsymbol{\eta}\right) - \boldsymbol{\eta}^T\boldsymbol{\eta} - \boldsymbol{\eta}^T\boldsymbol{J}\boldsymbol{z}w - \boldsymbol{\eta}^T\widetilde{\boldsymbol{z}}\right]. \tag{142}$$

Integration of the last equation in interval $(0, t)$ leads to

$$a^2(t) - a^2(0) = -\int_0^t \frac{d}{dt}\left(\boldsymbol{\eta}^T\bar{\bar{\boldsymbol{M}}}\boldsymbol{\eta}\right)dt - 2\int_0^t \boldsymbol{\eta}^T\boldsymbol{\eta}\,dt - 2\int_0^t \boldsymbol{\eta}^T\boldsymbol{J}\boldsymbol{z}w\,dt - 2\int_0^t \boldsymbol{\eta}^T\widetilde{\boldsymbol{z}}\,dt. \tag{143}$$

Consequently we have

$$a^2(t) - a^2(0) = -\boldsymbol{\eta}^T\bar{\bar{\boldsymbol{M}}}\boldsymbol{\eta} - 2\int_0^t \boldsymbol{\eta}^T\boldsymbol{\eta}\,dt - 2\int_0^t \boldsymbol{\eta}^T\boldsymbol{J}\boldsymbol{z}w\,dt - 2\int_0^t \boldsymbol{\eta}^T\widetilde{\boldsymbol{z}}\,dt + \boldsymbol{\eta}^T(0)\bar{\bar{\boldsymbol{M}}}(0)\boldsymbol{\eta}(0). \tag{144}$$

From the last equation we can write the following inequality

$$a^2(t) = a^2(0) + \boldsymbol{\eta}^T(0)\bar{\bar{\boldsymbol{M}}}(0)\boldsymbol{\eta}(0) - \boldsymbol{\eta}^T\bar{\bar{\boldsymbol{M}}}\boldsymbol{\eta} - 2\int_0^t \boldsymbol{\eta}^T\boldsymbol{\eta}\,dt - 2\int_0^t \boldsymbol{\eta}^T\boldsymbol{J}\boldsymbol{z}w\,dt - 2\int_0^t \boldsymbol{\eta}^T\widetilde{\boldsymbol{z}}\,dt \geqslant 0. \tag{145}$$

In fact scalar function $a(t)$ is defined by Eq. (145) under the condition that integrals which appear there are bounded. Note that first two elements in Eq. (145) are always positive and initial condition $a(0)$ of the differential equation given by (142) can be chosen positive and big enough. At the same time we can choose $a(0)$ big enough such that in Eq. (145) equal sign is not present. Of course $a(0)$ should be different from zero. We can easily calculate function $a(t)$ from expression (145) and check that the following differential equation is satisfied

$$\dot{a}(t) = \frac{\boldsymbol{\eta}^T\left(\boldsymbol{R} - \boldsymbol{J}\boldsymbol{z}w - \widetilde{\boldsymbol{z}}\right)}{a(t)}. \tag{146}$$

Additionally we have to assume that the integrals which appear in Eq. (145) are bounded. Therefore all negative terms which appear in Eq. (145) are bounded and as a consequence we can choose $a(0)$ such that r. h. s. of Eq. (145) is greater than zero. Conversely if we assume that the above signals are bounded we are able to choose proper $a(0)$ which satisfies Eq. (145).

The last equation but in different form was introduced by Galicki [11] (for rigid body manipulators). However a more detailed analysis of function $a(t)$ for mobile robots is given in this work. One can also notice that Eq. (146) can be interpreted as a kind of passivity which is present in mechanical systems. Still we get a global asymptotic stability since we can always find a proper initial value of $a(0)$ different from zero. Since signals $w(t)$, $\widetilde{\boldsymbol{z}}(t)$ and $\boldsymbol{\eta}(t)$ tend to zero asymptotically $a^2(t)$ is different from zero assuming that $\boldsymbol{\eta}(0) \neq \boldsymbol{0}$, which in practical applications is usually the case. From Eq. (145) it is clear that $a(t)$ has always the same sign and does not tend to zero. The quotient given by Eq. (146) is well defined and obviously $a(t)$ is bounded what we stated above. Note however that the quotient defined in Eq. (146) does not exist for any system. From the derivation described above we believe that it exists only for passive systems. Existence for other systems is not guaranteed whatsoever.

5. Simulation and experimental results

In this section we present some simulation results and preliminary experiments. Simulation results were carried out using *Matlab*® and *Simulink*® tools. In general, we did many different simulations; namely using only kinematic oscillator, kinematic oscillator and dynamic model and, finally using three levels of the proposed control scheme. Here we present only representative results, while a wide analysis of them

can be found in reference [15]. Kinematic oscillator has been used for both set point and trajectory control. For the purpose of simulation we assumed the following reference velocities $v_{r1} = 0.2[\frac{m}{s}]$ and $v_{r2} = 0.5[\frac{rad}{s}]$. Robot has to follow trajectory which is a circle of radius $0.4[m]$ located at the base coordinate system with its middle point $[x_0, y_0] = [0, 0.4]$. The starting point is defined as $[0\ 0\ 0]$. An auxiliary signal $\boldsymbol{z}_d(0) = [0.1061\ 0.1061]$. The coefficients which characterize the oscillator are as follows $k_1 = 100$, $k_2 = 100$, $\alpha_0 = 0.1$, $\alpha_1 = 0.5$ and $\varepsilon_1 = 0.05$. Reference (dotted line) and actual (continuous line) trajectories are presented in Fig. 5. The steady state

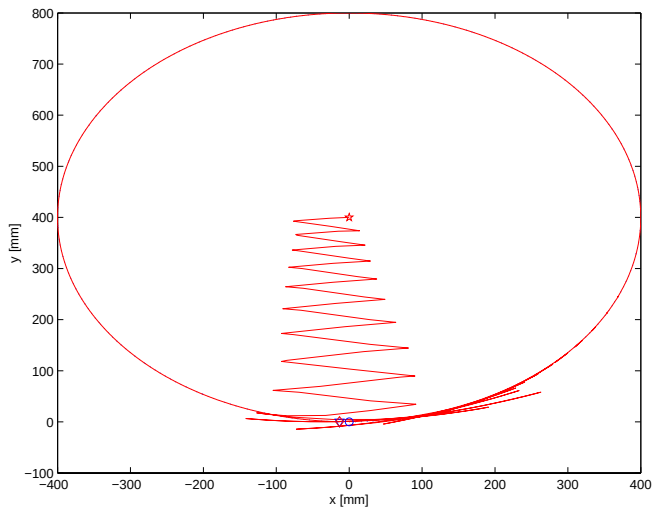

Figure 5. Reference and actual trajectory, $\varepsilon_1 = 0.05$.

errors for this simulation are as follows $|\widetilde{x}| = 0.3 \cdot 10^{-6}[mm]$, $|\widetilde{y}| = 4.8 \cdot 10^{-6}[mm]$, $|\widetilde{\theta}| = 2.8 \cdot 10^{-7}[^o]$. During the experiments it was observed that when $\varepsilon_1 > 0.5$ oscillator has a high dumping and the steady state errors have bigger values, while when $\varepsilon_1 < 0.5$ the tracking errors have smaller values. In the above experiment we assumed $d = 0$.

Next the simulation experiments were carried out with dynamic model of the robot itself. Here we assumed the following parameters of the robot $m_0 = 0.35[kg]$, $m_1 = 0.05[kg]$, $A_k = 0.23 \cdot 10^{-6}[kgm^2]$, $C_n = 0.1 \cdot 10^{-5}[kgm^2]$, $J = 0.4 \cdot 10^{-3}[kgm^2]$, $2R = 0.075[m]$, and $r = 0.0265[m]$. The results of this simulation experiments are shown in Figs. 7 and 8. The constant coefficients of the kinematic oscillator have the following values $k_1 = 7.5$, $k_2 = 10.25$, $\alpha_0 = 0.008$, $\alpha_1 = 1.0$, and $\varepsilon_1 = 0.8$. The desired velocities are as follows $v_{r1} = 0.15[\frac{m}{s}]$ and $v_{r2} = 0.25[\frac{rad}{s}]$. Recall that according to the theorem presented in the previous section the errors are asymptotically stable to values which are not zero. As a matter of fact the errors (both position and orientation) remain bounded. Numerical values of these errors are within $|\widetilde{x}| < 20[mm]$, $|\widetilde{y}| < 20[mm]$, and $|\widetilde{\theta}| < 1.2[^o]$. It can be observed that in the case of the two level control loop the proposed

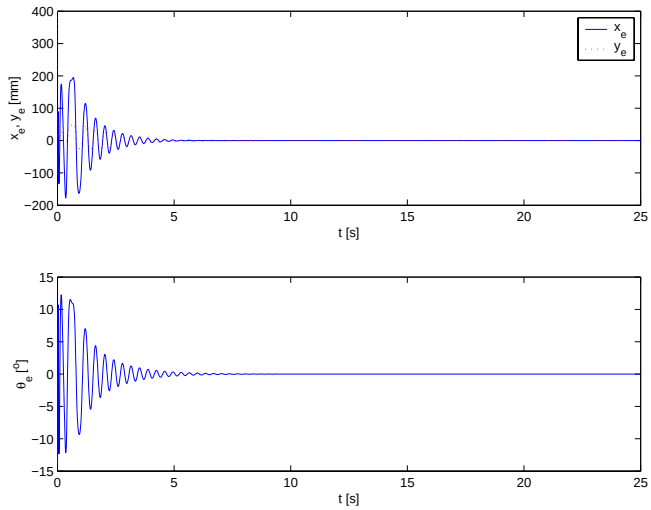

Figure 6. Position and orientation errors, $\varepsilon_1 = 0.05$.

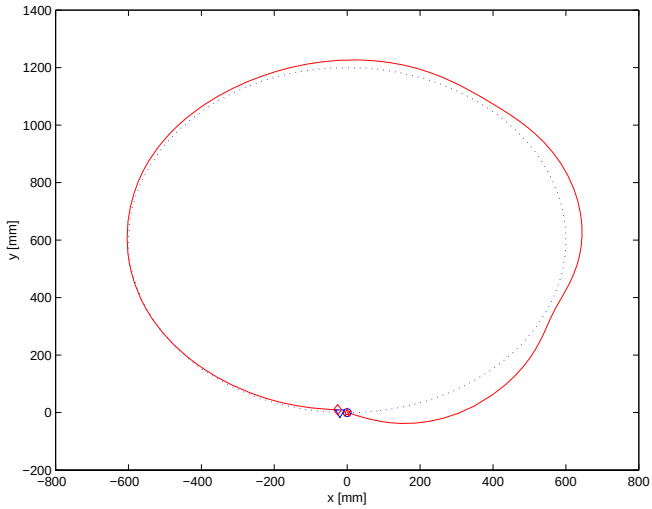

Figure 7. Reference and actual trajectory

algorithm is able to follow the reference trajectory. On top of that the signals seem to be more smooth, namely dynamics smooth out all signals in the system.

At the third level we show the simulation results of the final control algorithm which includes three levels of control, kinematic, dynamic and servo loop. In addition to the parameters listed above we introduce other parameters $L_a = 24 \cdot 10^{-3}[H]$,

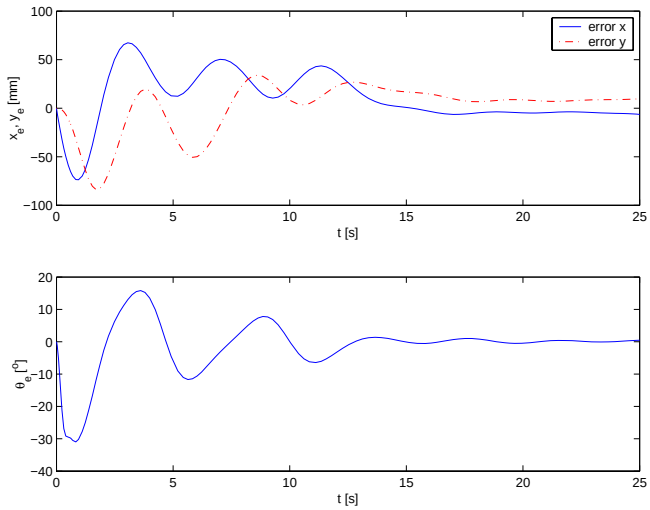

Figure 8. Tracking errors

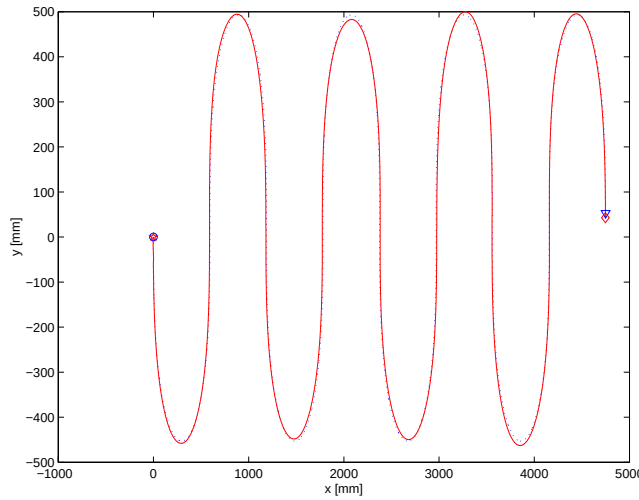

Figure 9. Reference and actual trajectory ($d = 0.02[m]$, $\varepsilon_1 = 0.8$)

$R_a = 11.3[\Omega]$, and $\tau_{max} = 1.36 \cdot 10^{-3}[Nm]$. Here it was assumed that the robot follows a sine trajectory and the reference velocities have the following values $v_{r1} = 0.2[\frac{m}{s}]$ and $v_{r2} = 0.785 \sin(0.5t)[\frac{rad}{s}]$. The simulation results are presented in Figs. 9 and 10. The parameters of the kinematic oscillator are as follows $k_1 = 30$, $k_2 = 50$, $\alpha_0 = 0.008$, $\alpha_1 = 1.0$, and $\varepsilon_1 = 0.8$. The three levels control algorithm was tested on several exam-

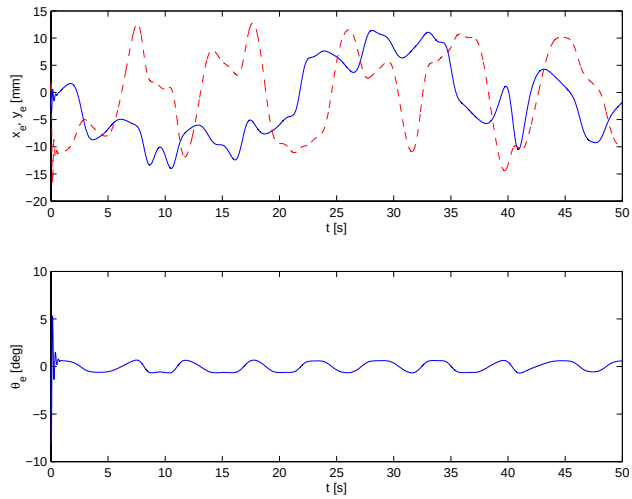

Figure 10. Trajectory tracking errors

ples which show that the position and orientation errors are within the following bounds $|\widetilde{x}| < 14[mm]$, $|\widetilde{y}| < 17[mm]$ and $|\widetilde{\theta}| < 8.0[^o]$.

In order to test the proposed algorithm experimentally we built a prototype of a mobile robot *Mini Tracker2*β, presented in Fig. 11. The control system of this robot consists of two microprocessor systems. Obviously the main program resides on a PC compatible computer. Communication between the host computer and robot computer is realized via fast RS232 IrDA. Robot weights $0.45[kg]$ and can move with maximum speed about $1[\frac{m}{s}]$ and acceleration about $0.5[\frac{m}{s^2}]$. Some preliminary results are shown in Figs. 12 and 13. Here robot is supposed to follow a sine trajectory (dotted line in Fig. 12) with the reference velocities $v_{r1} = 0.2[\frac{m}{s}]$ and $v_{r2} = 0.2 \sin t[\frac{rad}{s}]$. Actual trajectory in Fig. 12 is denoted by continuous line. At the moment the experimental results presented here are realized in open loop due to some difficulties of the communication between *Simulink*® and on-board computer via RS232C which works only in one direction, namely from the host computer to the on board computer. Position and orientation in Cartesian space were measured by the vision system which is installed above the plane on which mobile robot moves.

6. Concluding remarks

In this paper we proposed a three level control algorithm which is a backstepping type for trajectory tracking and set point control. The proposed control algorithm consists of kinematic, dynamic, and servo loop and uses the idea of kinematic oscillator. It was proven that the closed loop system is asymptotically stable to certain bounds of

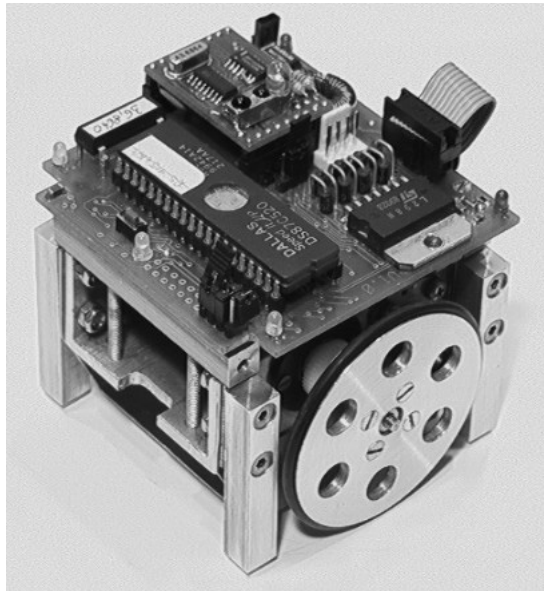

Figure 11. Mobile robot *Mini Tracker2β*

the tracking position and orientation errors. Notice that the second theorem is satisfied under the condition that certain integrals which appear in Eq. (145) are bounded. This condition is rather strong and one can think how to alleviate it which is still under consideration. Simulation results illustrate the theoretical considerations. Some experimental work is presented too. In the near future more experimental work will be done. Preliminary work which uses an idea of Morin and Samson [20], [22] of kinematic controller was done and it would be extended to the dynamics and servo loop level. The initial results look promising and we strongly believe that it is worth to continue this research.

Authors would like to thank Prof. Krzysztof Tchoń for his valuable comments and suggestions which improved final version of this paper.

References

[1] A. ASTOLFI: Asymptotic stabilization of nonholonomic systems with discontinuous control. *Ph.D. Thesis*, Swiss Federal Institute of Technology, Zurich, 1996.

[2] B. D'ANDREA-NOVEL, G. CAMPION and G. BASTIN: Control of nonholonomic wheeled mobile robots by state feedback linearization. *Int. J. of Robotics Research*, **14**(6), (1995), 543-559.

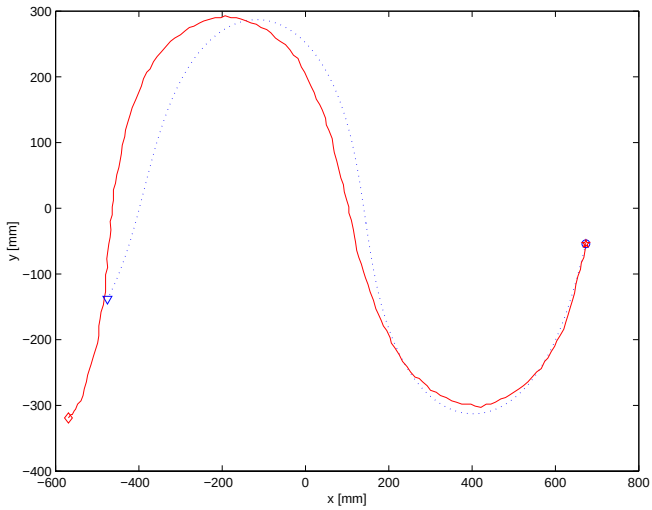

Figure 12. Reference and actual trajectory.

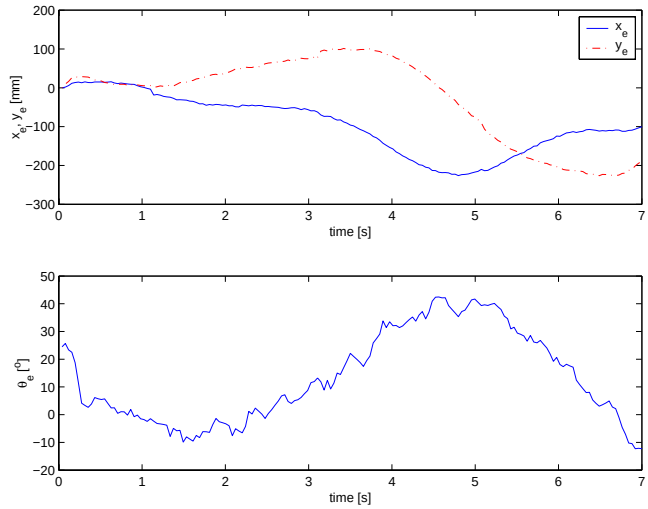

Figure 13. Position and orientation errors

[3] L. BEJI and Y. BESTAOUI: A tracking control method of mobile robot with kine-dynamics considerations. *Proc. of the 5th IFAC Symposium*, NOLCOS, (2001).

[4] Y. BESTAOUI: An optimal velocity generation of a rear wheel drive tricycle along a specified path. *Proc. of the American Control Conf.*, (2000), 2907-2911.

[5] R. W. BROCKETT: Asymptotic stability and feedback stabilization. In *Differential Geometric Control Theory*, R. W. Brockett, R. S. Milman and H. J. Susmann (Eds), Birkhauser, Boston, (1983), 181-191.

[6] G. CAMPION, B. D'ANDREA-NOVEL and G. BASTIN: Controllability and feedback stabilization on nonholonomic mechanical systems. In C. Canudas de Wit, (Ed), *Lecture notes in Control and Information, Proc. of the IEEE Int. Conf. on Robotics and Sciences*, Springer-Verlag, (1991), 106-224.

[7] W. E. DIXON and D. M. DAWSON: Global exponential set point control of wheeled mobile robots; a Lyapunov approach. *Automatica*, **36** (2000), 1741-1746.

[8] W. E. DIXON, D. M. DAWSON, F. ZHANG and E. ZERGEROGHE: Global exponential tracking control of a mobile robot system via a PE condition. *IEEE Trans. on Systems, Man and Cybernetics - Part B: Cybernetics*, **30**(1), (2000), 129-142.

[9] W. E. DIXON, D. M. DAWSON, E. ZERGEROGLU and F. ZHANG: Robust tracking and regulation control for mobile robots. *Int. J. of Robust and Nonlinear Control*, **10** (2000), 199-216.

[10] R. FIERRO: A hybrid system approach to a class of intelligent control systems. *Ph.D. Thesis*, The University of Texas at Arlington, 1997.

[11] M. GALICKI; Robust Tracking of manipulators subject to control constraints. *Studies in Automation and Information Technology*, **25** (2000), 83-93 (in Polish).

[12] A. ISIDORI: Nonlinear Control Systems. 2nd edition, Springer-Verlag, 1989.

[13] H. K. KHALIL: Nonlinear Systems. 2nd edition, Prentice-Hall, 1995.

[14] I. KOLMANOVSKY and N. HARRIS MCCLAMROCH: Developments in nonholonomic control problems. *IEEE Control Systems*, (1995), 20-36.

[15] K. KOZŁOWSKI and J. MAJCHRZAK: Steering of a nonholonomic mobile robot using a kinematic oscillator. *Proc. of the National Conference on Robotics*, (2001), 31-44 (in Polish).

[16] TI-CHUNG LEE, KAI-TAI SONG, CHING-HUNG LEE and CHING-CHENG TENG: Tracking control of unicycle-modeled mobile robots using a saturation feedback cantroller. *IEEE Trans. on Control Systems Technology*, **9**(2), (2001), 305-318.

[17] M. KRISTIĆ, I. KANELLAKOPOULOS and P. KOKOTOVIĆ: Nonlinear and adaptive control design. John Wiley & Sons, Inc. 1995.

[18] R. MARINO and P. TOMEI: Nonlinear Control Design, Geometric, Adaptive and Robust. Prentice Hall, 1995.

[19] A. MAZUR: Control algorithms for the kinematics and dynamics of mobile manipulators: a comparative study. *Archives of Control Sciences*, **11**(3/4), (2001), 223-244.

[20] P. MORIN and C. SAMSON: A characterization of the Lie Algebra Rank Condition by transverse periodic functions. *Proc. of the IEEE Conference on Decision and Control*, (2000), 3988-3993.

[21] P. MORIN and C. SAMSON: Feedback control of nonholonomic wheeled vehicle. *Archives of Control Sciences*, **12**(1/2), (2002), 7-36.

[22] P. MORIN and C. SAMSON: Practical stabilization of a class of nonlinear systems. Application to chain systems and mobile robots. *Proc. of the IEEE Conference on Decision and Control*, (2000), 2989-2994.

[23] L. PALOPOLI, F. CONTICELLI and B. ALLOTTA: Multi-level stabilizing control of an nonholonomic vehicle and its discrete-time multirate implementation. *IEEE Int. Conf. on Robotics and Automation*, (2000), 1830-1836.

[24] J. B. POMET: Explicit design of time-varying stabilizing control laws for a class of controllable systems without drift. *Systems and Control Letters*, **18** (1992), 147-158.

[25] C. SAMSON: Time-varying feedback stabilization of car-like wheeled mobile robots. *Int. J. of Robotics Research*, **12** (1993), 55-64.

[26] C. SAMSON: Velocity and torque feedback control of an nonholonomic cart. *Int. Workshop in Adaptive and Nonlinear Control; Issues in Robotics*, (1990), 125-151.

[27] D. J. SFIRDELEN: Feedback control of nonholonomic mobile robots. *Ph.D. Thesis*, Department of Engineering Cybernetics, The Norwegian Institute of Technology, 1993.

[28] K. TCHOŃ, A. MAZUR, I. DULĘBA, R. HOSSA and R. MUSZYŃSKI: Robot manipulators and mobile robots: Models, Trajectory Planning, Control. Akademicka Oficyna Wydawnicza PLJ, Warsaw, 2000, (in Polish).

[29] JUNG-MIN JONG-WAN KIM: Sliding mode motion control of nonholonomic mobile robots. *IEEE Control Systems*, (1999), 15-23.

[30] Y. YAMAMOTO and X. YUN: Coordinating locomotion and manipulation of a mobile manipulator. *IEEE Trans. on Automatic Control*, **39**(6), (1994), 1326-1332.

[31] B. J. YOUNG, J. R. LAWTON and R. W. BEARD: Two hybrid control schemes for nonholonomic robots. *Proc. of the IEEE International Conference on Robotics and Automation*, (2000), 1824-1829.